CHAPTER IV
DIELECTRIC PROPERTIES AT MICROWAVE FREQUENCY IN BARIUM STRONTIUM TITANATE/POLY(BENZOXAZINE/URETHANE) COMPOSITES

4.1 Abstract

Poly(benzoxazine/urethane) composites were firstly prepared as a new type of dielectric material with attractive dielectric behaviors. In this work, the toughness of polybenzoxazine was enhanced by adding urethane elastomer (PU). The 90/10 vol.% of BA-a/PU copolymer was suitable for being used as a polymer matrix owing to numerous outstanding characteristics such as excellent dielectric properties, high thermal stability, and good flexibility. To uplift the dielectric constant, barium strontium titanate (BST) in the form of $Ba_{0.3}Sr_{0.7}TiO_3$ was combined as a ceramic filler prepared via sol-gel technique to formulate the composition. The effects of BST loading on microwave dielectric properties were studied at temperatures ranging from -50 °C to 150 °C in a frequency range of 300 MHz to 1 GHz. The dielectric constant of the composites was increased with increasing filler ratio. The incompatibility of polymer-ceramic composites was also improved by surface treatment on BST using 3-aminopropyl-trimethoxysilane and benzoxazine/urethane mixture. It was found that the surface modification on BST nanoparticles was effective to disperse BST nanopowders in the polymer matrix. The composite at 60 wt.% of BST treated by silane coupling agent had the highest dielectric constant (13.9) with a low dissipation factor (0.0095). The dielectric behaviors of all components were nearly stable at observed temperatures and frequencies. With the prominent characteristics as described, poly(benzoxazine/urethane) composites have potential applicability as high-performance dielectric materials in modern electrical industries.

Keyword: Poly(benzoxazine/urethane)composites; barium strontium titanate (BST); dielectric materials; microwave frequency

4.2 Introduction

New generation of microelectronic packaging such as capacitor applications has been focused on a high performance material being workable at microwave frequency. The obvious properties to manufacture one should exhibit appropriate dielectric constant, low dielectric loss for keeping the signal integrity, superb mechanical properties, and inexpensive raw materials [1]. It is a challenge for production to acquire all of these properties. By coupling different types of materials between polymer and ceramic can be an optional method [2]. There are a number of successfully prepared high performance polymer/ceramic composites for electronic applications in the last decade such as composites of polyimide, polyphenylene sulfide, epoxy, silicon-rubber, polyvinylidene difluoride [3-8]. For previous studies, the dielectric characteristics of aniline-based polybenzoxazine/BST composites are considerably attractive. The observed dielectric constants of the composites at 1 MHz were in the range of 35-40 with less than 0.12 of loss tangent [9]. Evidently, one of major problems in this regard is to the brittleness of the cross-linked resins, which limits the industrial production. With concerning the versatile performances, polymer alloys have received increasing attention from both the scientific and industrial communities as it is widely accepted as an efficient method to offer superior properties to the development of entirely new materials. Several polymers such as urethane elastomer, epoxy, poly(ε-caprolactone), and polydimetylsiloxane have been proposed to alloy with benzoxazine resins [10-12]. Among these combinations, benzoxazine-urethane copolymers with the single glass transition temperature exhibited interesting features such as the improvement in toughness, enhancing glass transition temperature and ease of processing [13]. As a result, the benzoxazine/urethane composites were performed in this work. For this purpose, poly(propylene glycol), tolylene 2,4-diisocyanate terminated (PPG-TDI) as urethane prepolymer was combined with aniline-based benzoxazine monomer (BA-a) at various weight ratios. The suitable composition of the alloyed was selected in order to use as a polymer matrix. Additionally, benzoxazine/urethane composites were fabricated using $Ba_{0.7}Sr_{0.3}TiO_3$ filler with the incorporation of surface modification, i.e. 3-aminopropyl-trimethoxysilane and benzoxazine/urethane mixture. The

dielectric properties as functions of ceramic loadings at microwave frequency, from -50 °C to 150 °C, were investigated and discussed. The calculation based on several commonly used models was also studied in order to predict the relative permittivity behaviors of the composite.

4.3 Experimental

4.3.1 Synthesis of Aniline Based Benzoxazine Monomer

The synthesis of aniline-based benzoxazine monomer was prepared via the reaction of bisphenol A, paraformaldehyde and aniline at the molar ratio of 1:4:2, respectively through solventless method as shown in Figure 4.1. The combination of raw materials was heated to 110°C for 30 min. The obtained viscous solution with high yellow was cool down and ground into powder. Then the final product was further purified in order to remove any unreacted starting materials. The powder was washed at least 3 times by using cool methanol and dried before used.

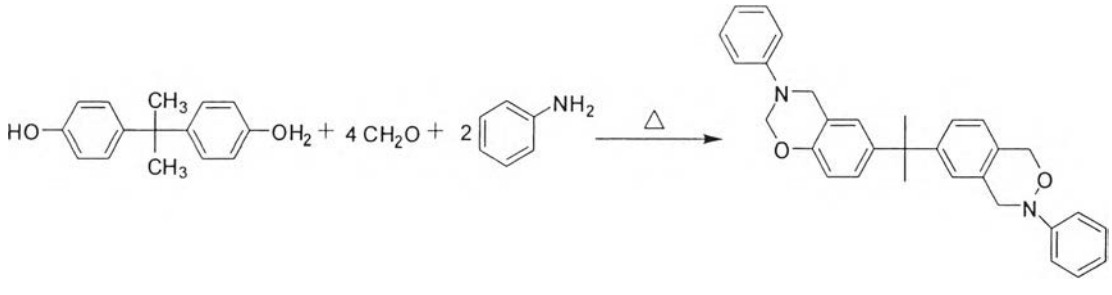

Figure 4.1 Synthesis of aniline-based benzoxazine monomer (BA-a) [14]

4.3.2 Preparation of poly(benzoxazine/urethane) specimens

The benzoxazine monomer (BA-a) was blended with the poly(propylene glycol) tolyene 2,4-diisocysnate terminated as urethane prepolymers (PU) to provide BA-a/PU mixtures. The fraction of urethane prepolymer was varying at 0, 10, 20, 30, and 50 vol. %. The mixture was then heated to about 120°C for 20 min. without solvent in aluminum pan and mixed until a homogeneous mixture was obtained. The molten resin mixture was poured into an aluminum mold and step cured in an air-circulated oven at 150 °C for 30 min., 170 °C for 30 min., and 200 °C

for 2 hr. The vacuum was also applied in order to help reduce porous in the specimens. Part of the mixture was taken for differential scanning analysis. The color of the cured samples changed from yellow to dark brown during the crosslinking process. The specimen was finally left to cool down to room temperature and was then ready for material characterizations.

4.3.3 Preparation of Barium Strontium Titanate by Sol-Gel Process

To prepare barium strontium titanate, $Ba_{0.3}Sr_{0.7}TiO_3$ (BST), 0.3 mole of barium acetate and 0.7 mole of strontium acetate were separately dissolved in glacial acetic acid, followed by the addition of methanol to each solution. Both of the completely soluble components were mixed together and then an equimolar amount of titanium (iv) n-butoxide was added into this mixture under vigorous stirring. After gel was formed, it was calcined by 2-step thermal decomposition to decompose the solvent and crystallize the BST powder. The calcination procedure is shown in Figure 4.2.

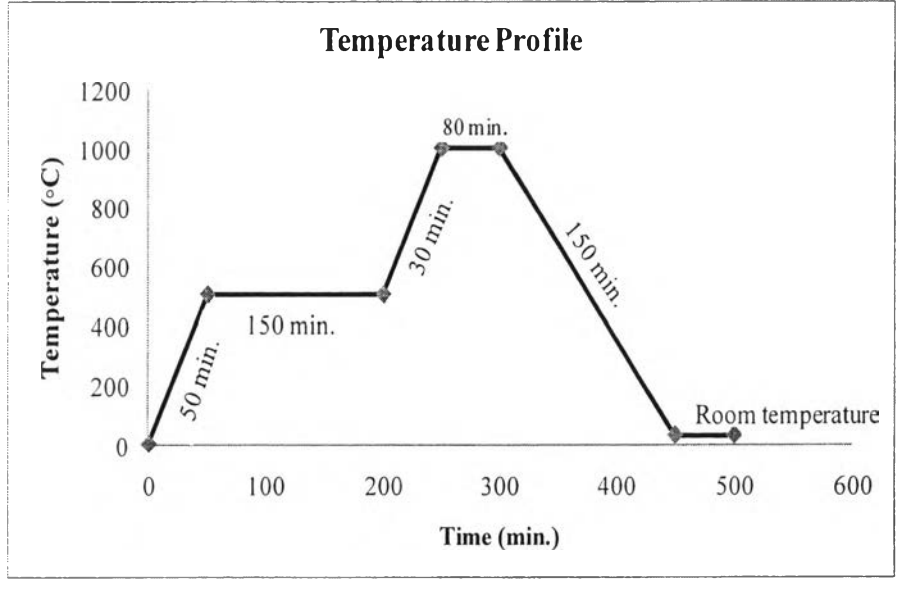

Figure 4.2 The temperature profile for two-step thermal decomposition of BST.

4.3.4 Composite Preparation

For composite fabrication, at 90/10 vol.% of BA-a/PU copolymer as a polymer matrix and BST ceramic ($Ba_{0.3}Sr_{0.7}TiO_3$) were mixed together by varying BST content at 30, 40, 50, and 60 wt.% through melt mixing method to avoid phase separation. After that, the mixtures was prepared as composite specimens with the thickness of 1 mm. and 20 mm. in diameter with curing conditions which given in 4.3.2

4.3.5 Surface Modification of BST Powders

4.3.5.1 Surface Modification by Silane Coupling Agent

The 3-aminopropyl-trimethoxysilane (2 g) was dissolved in 5:95 ml of ethanol-water solution. Subsequently, the 40 g of BST powder was added into the mixure. This suspension was further dispersed in an ultrasonic chamber at room temperature for 10 min. and stirred at 70°C for 1 h. The colloidal solution was centrifuged and later washed off the residual by ethanol. After dried in a vacuum oven at 50°C, the silane treated BST particles were obtained.

4.3.5.2 Surface Modification by BA-a/PU copolymer

The 5 wt.% of BA-a/PU copolymer at 90/10 vol.% was dissolved in THF. The prepared solution was slowly added dropwise to stirring BST particle/THF slurry system. Then the mixture was continuously stirred for 1 h. and evaporated THF out at 70°C. Lastly, BA-a/PU copolymer treated BST was dried in a vacuum oven overnight in order to remove the residual solvent.

4.3.6 Characterizations and testing

The molecular structures of the aniline-based benzoxazine monomer were confirmed by nuclear magnetic resonance spectrometer (Varian Mercury NMR spectrometer). The ^{1}H-NMR spectrum was recorded at 400.00 MHz of operation by using deuterated chloroform ($CDCl_3$) as a solvent. The functional groups of benzoxazine monomer, benzoxazine/urethane copolymer and BST powder including modified BST by surface treatment were observed by using a Nicolet Nexus 670 FTIR spectrometer in the frequency range of 4000-400 cm^{-1} with 64 scans at a

resolution of 2 cm^{-1}. The potassium bromide (KBr) pellet technique was applied in the preparation of sample powder. To determine the particle size of BST powder, transmission electron microscopy (TEM) performed on Hitachi/S-4800 electron microscope with an accelerating voltage of 100 kV was performed. The curing behaviors of both benzoxazine based and benzoxazine/urethane resin mixtures were studied by using differential scanning calorimeter (Perkin-Elmer DSC 7). The samples were weighted at approximately 4-10 mg and put in an aluminum pan with lid. The scanning condition was at 5 °C/min. of heating rate from 30 °C to 300 °C under 25 ml/min. of N_2 purging. The crystal phase of the present BST composition was studied with X-Ray Diffractometer Model D8 Advance: Bruker AXS, Germany with Cu target at wavelength = 1.5406 angstroms. Transmission electron microscopy performed on Hitachi/S-4800 electron microscope with an accelerating voltage of 100 kV was carried out to examine the crystallite phase of BST powder. The density of BST powder, polybenzoxazine, and poly(benzoxazine/urethane) based was determined by gas pycnometer (Quantachrome, Ultrapycnometer 1000) under helium purge at pressure of 20 psi. According to ASTM D 792-00, the relative density of the polymer blends and the composites were measured by following its test method A to observe the presence of porosity. The apparatus equipped with Balance SARTORIUS research RC210S and kit SARTORIUS YDK201. The 20 mm × 5 mm × 2 mm sample was weighed in air, and then weighed when it was completely immersed in deionized water. The weight was again noted after the sample was removed and wiped of excess water. The density of the specimen was lastly obtained by calculation. To observe glass transition temperature (T_g) of materials and mechanical properties, dynamic mechanical analysis (DMA) was performed by using GABO EPLEXOR 100 N. The test was measured in a three-point bending mode. For temperature sweep experiment, 1 Hz of frequency and 0.1% of strain value were applied. The temperature was scanned from -100 °C to 250 °C for PBA-a/PU alloys and from 25 °C to 250 °C for PBA-a/PU composites with a heating rate of 2 °C/min under nitrogen atmosphere. Thermogravimetric analysis (TGA) was conducted on a Perkin-Elmer Pyris Diamond TG/DTA instrument at a heating rate of 10 °C min^{-1}. This condition with approximately 5 mg of sample loaded was flowed under N_2 with flow rate of 100 ml/min. For the

dielectric study, the surfaces of the cured benzoxazine , benzoxazine/urethane alloys and the composites (1 mm thick and the 2 cm in diameter) were polished on both sides for dielectric characterization. Measurement of the dielectric properties (dielectric constant (ε'), and loss tangent ($\tan\delta$; $\varepsilon''/\varepsilon'$)) was taken with an E4991A RF Impedance/Material Analyzer equipped with a 16453A dielectric material test fixture, Agilent Technologies, Inc., USA) at a frequency range of 300 MHz to 1 GHz. The prepared sample was placed inside a Espec SU-261 temperature chamber (variable temperature oven). The temperature was controlled from -50 °C to 150 °C by first heated from room temperature to 150 °C and then cool down at 10 °C increments until reaching -50 °C. The computer was programmed to collect data at each step during the temperature ramp down. Microstructure and surface morphology analyses of BST powders and the composites were done by using a scanning electron microscope (SEM; HITACHI S-4800) at voltage of 15 kV. Atomic force microscope performed on XE-100 Series Park Systems SPM Controller with force modulation mode, at 10 μm of scan size. and at 0.2 Hz. of scan rate was used to observe microphase of copolymers.

4.4 Results and Discussions

4.4.1 Benzoxazine Monomer, Urethane Prepolymer and (Benzoxazine/Urethane) Copolymers Characterizations

4.4.1.1 Nuclear Magnetic Resonance Spectroscopy (NMR) Analysis

The molecular structure of BA-a monomer was confirmed by using ^{1}H NMR technique. The ^{1}H NMR spectra are seen in Figure 4.3

For BA-a monomer, multiplets peak of aromatic proton indicates at around 6.7-7.3 ppm. Characteristic peaks of methylene (O-CH_2-N) and methylene (Ar-CH_2-N) of oxazine ring are found at 5.35 and 4.6 ppm, respectively. Furthermore, the methyl proton of bisphenol A (-CH_3) is observed at 1.6 ppm. The purification of the monomer can be indicated from ^{1}H NMR spectra which is no peaks of methylene groups from the oligomers (oxazine ring-opening process) at 3.10 and 3.60 ppm [14].

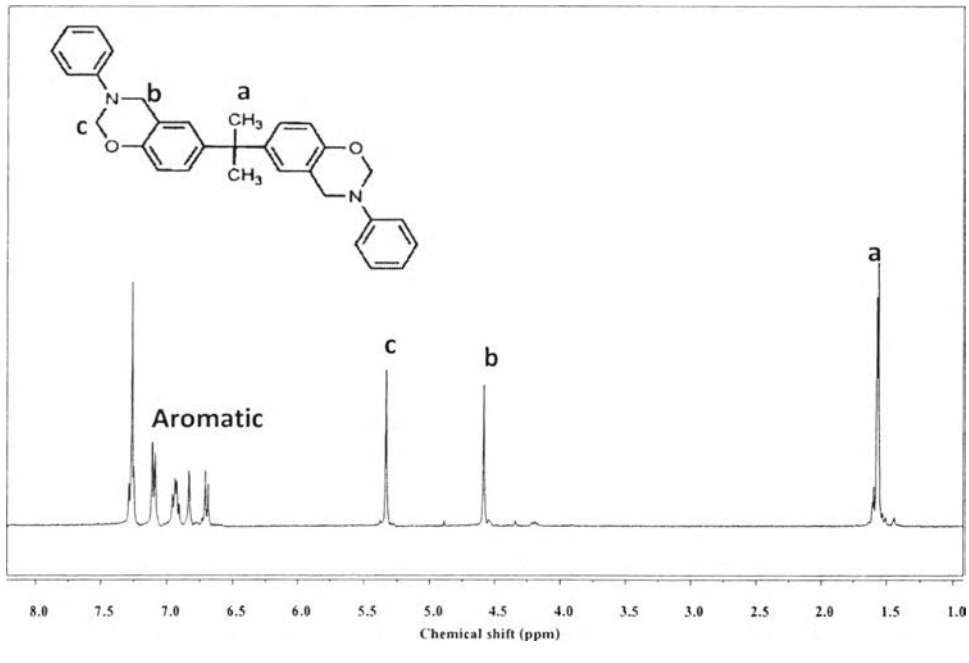

Figure 4.3 The ^{1}H-NMR spectrum of the aniline-based benzoxazine monomer (BA-a).

4.4.1.2 Fourier Transform Infrared Spectroscopy (FTIR) Analyses

Aniline-based benzoxazine monomer (BA-a), urethane prepolymer (PU), and BA-a/PU copolymer at 90/10 vol.% were characterized by using FTIR spectrometer to confirm their functional groups. The FTIR spectra of BA-a, PU, and at 90/10 vol.% of BA-a/PU mixture are shown in Figure 4.4, 4.5, and 4.6 respectively.

The FTIR spectrum of BA-a shows the tri-substituted benzene ring mode of oxazine ring structure at 1496 cm^{-1}. The antisymmetric C-N-C stretching mode can be indicated in the absorption band around 1240-1020 cm^{-1} whereas the symmetric mode appears at 830-740 cm^{-1}. The bands around 1240-1210 cm^{-1} and 1040-1020 cm^{-1} indicate the antisymmetric and symmetric C-O-C stretching modes, respectively. Additionally, CH_2 wagging of oxazine appears around 1360-1380 cm^{-1} and the band between 960 and 920 cm^{-1} also attributes to the benzene with an attached oxazine ring modes [15].

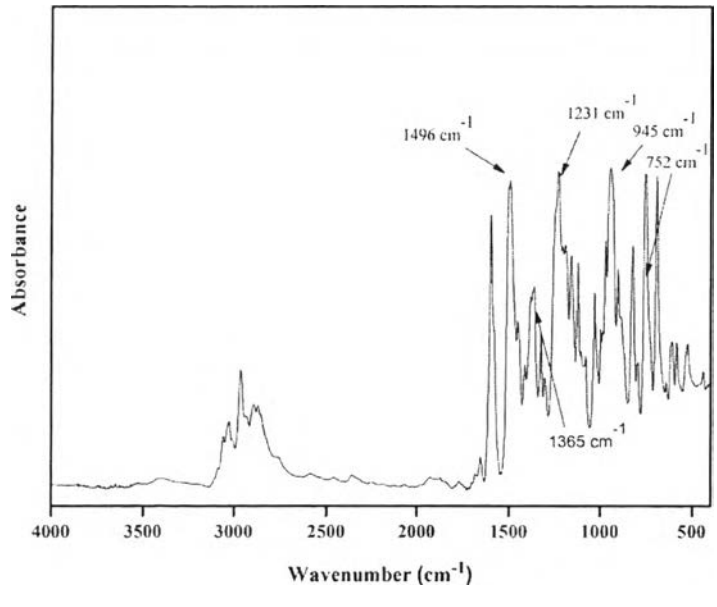

Figure 4.4 The FTIR spectrum of aniline-based benzoxazine monomer (BA-a).

The functional group of PU was observed for further assessing the acquisition of polymer alloys. The unique absorption peaks assigned to C=O

stretching of urethane and N=C=O stretching of unreacted-isocyanate group are found at 1729 and 2275 cm^{-1}, respectively [16].

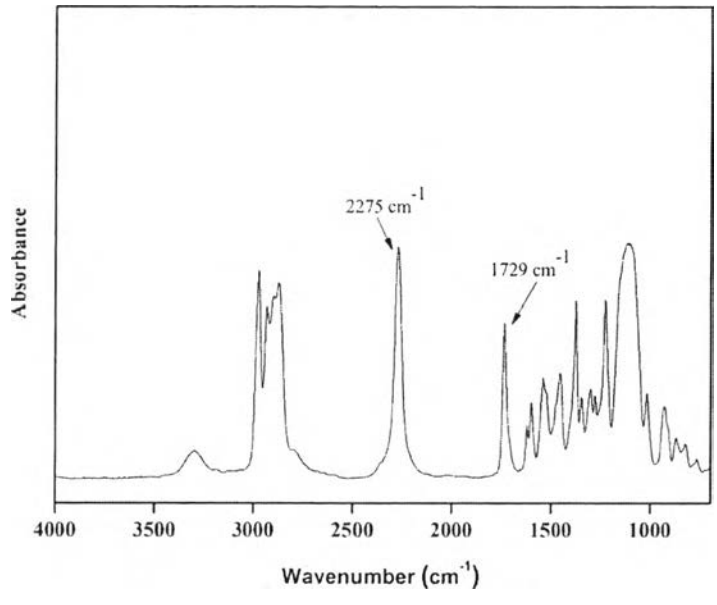

Figure 4.5 The FTIR spectrum of urethane prepolymer (PU).

To prepare BA-a/PU copolymers, at 90/10 vol.% of BA-a/PU mixture is a representative of samples to observe the functional groups of the binary system. A broad intensive IR absorption band appears around 3300-3600 cm^{-1} after cured at 150 °C for 30 min. followed by 170 °C for 30 min. The evidence indicates that phenolic hydroxyl group of benzoxazine monomers is generated by thermally polymerized through their ring opening reaction. However, this band is slightly week resulting from some parts of phenolic OH groups completely reacting with NCO groups of PU prepolymers. It is obviously noticed that the disappearance of absorbance at 2275 cm^{-1} is occurred after heated. On the other hand, the absorbances placed at 1620 and at 1536 cm^{-1} are also found, assigned to the secondary amide in the urethane groups. After the curing process, the absorptions at 945 and 1492 cm^{-1} represented the tri-substituted benzene ring in BA-a are weakened and the peak at 945 cm^{-1} (C-O-C bond) shifted to 957 cm^{-1}, which suggests a decrease in the tri-substituted benzene rings, indicating the ring-opening polymerization. Those absorbances do not completely disappear due to the existence of the tri-substituted

benzene ring in PU. Therefore, it may conclude that the reaction between NCO in PU and phenolic hydroxyl groups in the BA-a polymer might have occurred. Although not all the chemical changes can be confirmed by IR owing to the structural similarity of the PU and BA-a polymer. For more investigation of the curing behavior of benzoxazine monomer in the presence of the PU prepolymers, the materials would be characterized by DSC technique [17-18].

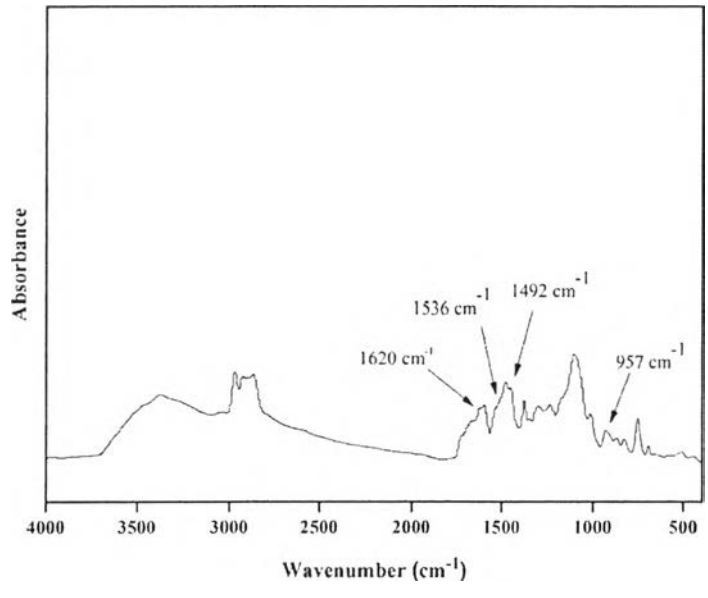

Figure 4.6 The FTIR spectrum of benzoxazine resin (BA-a) and PU (90/10 vol.%) thermally treating program at 150 °C for 30 min. followed by 170 °C for 30 min.

4.4.1.3 Differential Scanning Calorimetry (DSC) Analysis

DSC analysis was performed to monitor the neat BA-a monomer and the binary mixture system between benzoxazine monomer (BA-a) and urethane prepolymer (PU) on the curing behaviors as seen in Figure 4.7.

The studied compositions were observed at 100/0, 90/10, 80/20, 70/30, 60/40 and 50/50 vol.% of (BA-a/PU). It is obviously seen that the exothermic peaks of the pure BA-a and the mixtures show single transition of curing process. These characteristics of copolymers reveal the concurrently forming of network structure at the equivalent temperature range. The curing temperature of the neat

benzoxazine is located at 229 °C whereas the exothermic peaks of BA-a : PU mixtures at 90 : 10, 80 : 20, 70 : 30, 60 : 40, and 50:50 volume ratios are 235, 238, 241, 245, and 247 °C, respectively. In basis, the reactions between BA-a : PU consist of two reactions: the first reaction is the exothermic curing peak of the reaction between BA-a and BA-a, while the second one should be the reaction between the isocyanate group of the urethane prepolymer and phenolic hydroxyl group of the polybenzoxazine. The second reaction would generate after the phenolic hydroxyl group from ring opening of the benzoxazine monomer is formed. Therefore, exothermic peaks of the curing reaction tend to shift to a higher temperature when the volume fraction of urethane prepolymers in the copolymers increases. The thermograms also illustrate that the decrease in the area under the curing reaction peaks of the binary mixtures when the amount of all urethane prepolymers increase. This evidence attributes to the change from the BA-a : BA-a interaction to the BA-a : PU interaction with increasing the PU fraction in the copolymers. The exothermic heat reaction of BA-a : PU mixtures at 100:0, 90 : 10, 80 : 20, 70 : 30, 60:40 and 50 : 50 mass ratios are 234, 213, 172, 166, 153, and 96 J/g, respectively. The reduction of the curing exotherms with the PU infers the reaction between BA-a and PU, which generates a lower heat of interaction per mole of the reactants. However, excessive amount of the PU in the binary mixtures might also lead to the presence of the unreacted PU in the fully cured copolymers, and then the systematic decrease in the heat of reaction [18].

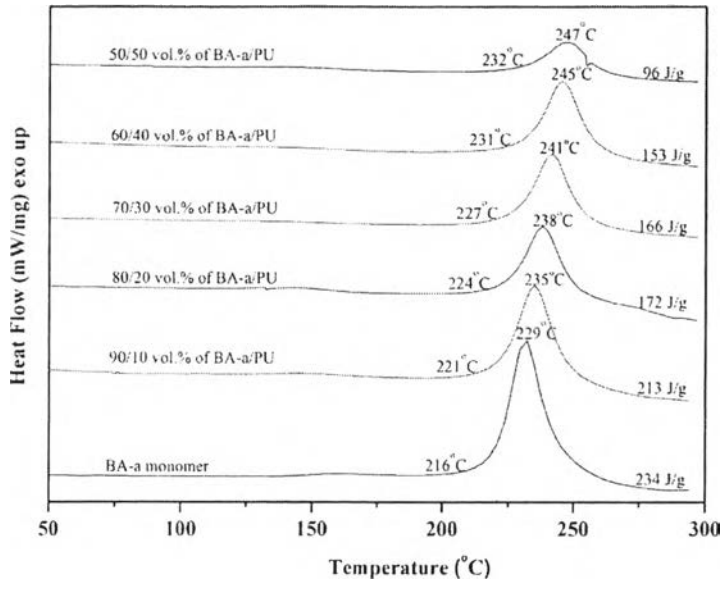

Figure 4.7 DSC patterns of BA-a/PU at various compositions: 100/0, 90/10, 80/20, 70/30, 60/40, 50/50 vol.%.

4.4.1.4 Microwave Dielectric Properties Measurements

Benzoxazine/urethane alloys (BA-a/PU) at difference urethane contents (0, 10, 20, 30, 40, and 50 vol.%) were investigated for dielectric behavior as a function of temperature in the range of -50 °C to 150 °C observed at 1 GHz. Figure 4.8a shows the dielectric constant of benzoxazine/urethane alloys and loss tangent is displayed in Fig. 4.8b.

(a)

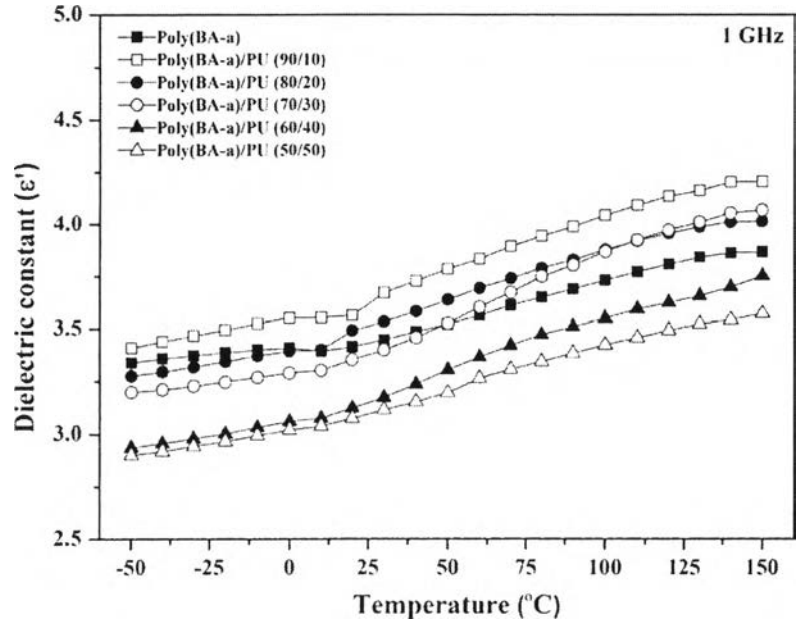

(b)

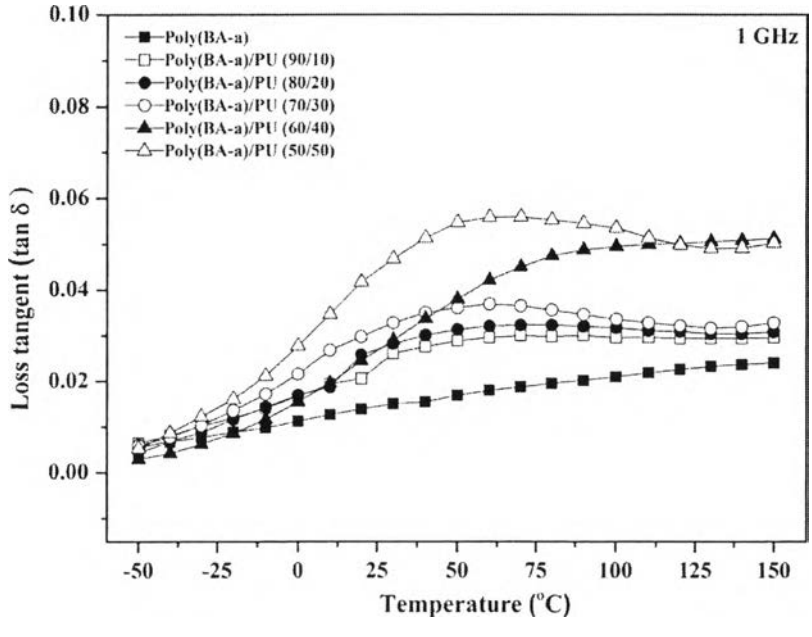

Figure 4.8 Temperature dependence of a) dielectric constant and b) loss tangent of BAa-a/PU alloys by varying urethane contents measured at 1 GHz.

In addition, Fig. 4.9 (a,b) shows the dielectric properties of cured BA-a/PU under frequency variation in the range of 300 MHz-1 GHz at room temperature.

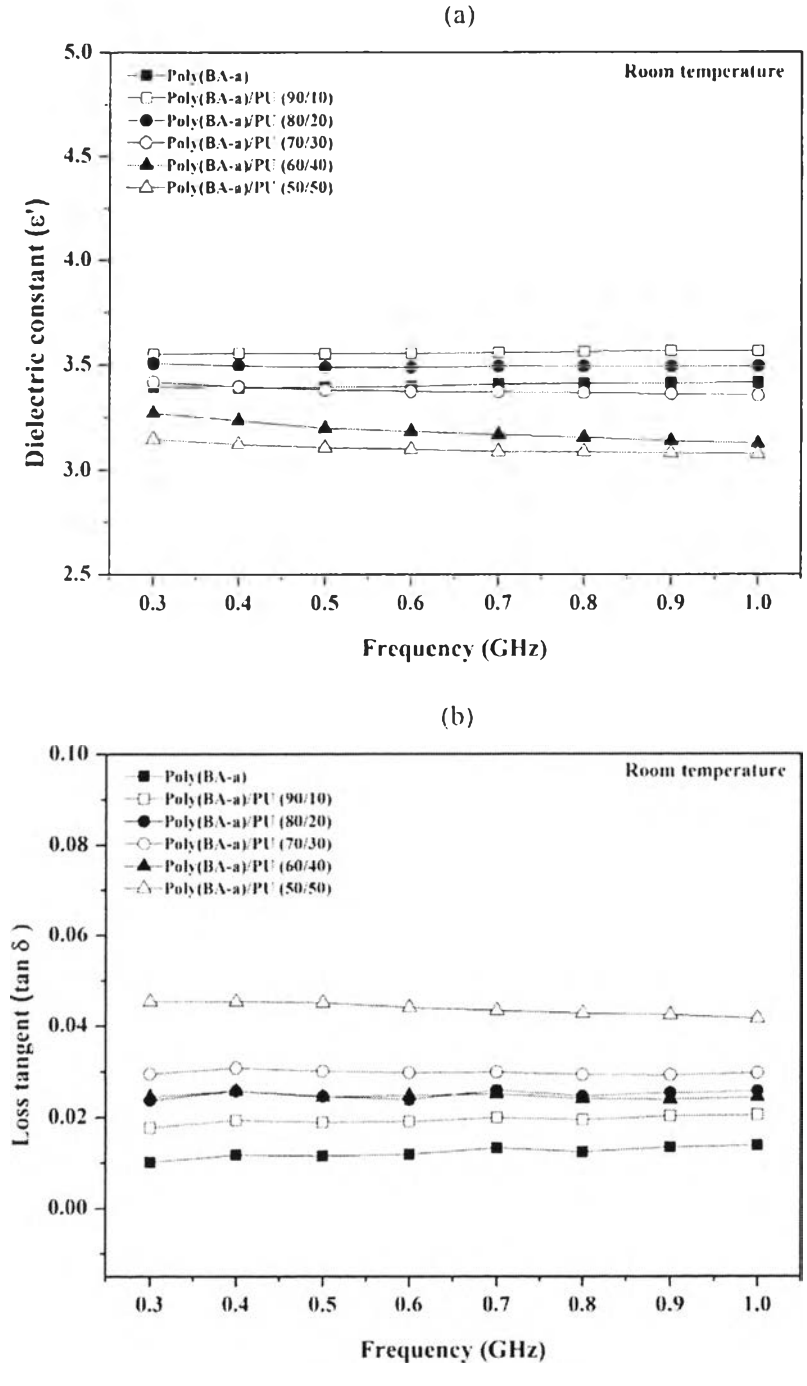

Figure 4.9 Frequency dependence of a) dielectric constant and b) loss tangent of BAa-a/PU alloys by varying urethane contents measured at room temperature.

The dielectric constant of the polymer matrix is dominantly improved with the addition of a small amount of PU. At 90/10 (vol.%) of BA-a/PU has the highest value of dielectric constants (ε') after observed at various temperatures. Therefore, this formula is more acceptable for being selection as a polymer matrix for the composite. The maximum relative permittivity of 90/10 vol.% of BA-a/PU appears at 150 °C and is as high as 4.21, which is greater than the neat polybenzoxazine (3.86). It can be inferred that a small amount of PU could induce more electronic polarization. To obtain a higher dielectric constant, by enhancing polarizability of the molecules, the small amount of PU is needed to the copolymer. Moreover, the gap between the highest and the lowest value of the dielectric constant under temperature variation of the polymer matrix does not exceed 1. The study of frequency dependence which is one of the most significant factors was also studied for describing the performance of polymers. After observed the dielectric properties, it is evident that the relative permittivity and dissipation factor exhibit a flat line neither significant rising nor falling in frequency deviation, which indicates that this polymer matrix is nearly stable in the fluctuation atmosphere. This characteristic of the copolymers stems from the normal high glass transition temperature (T_g). According to the Rimdusit report, T_g of polybenzoxazine is around 166 °C and shifts to higher temperatures when combined with polyurethane [13]. Another observation, it is found that a large urethane adding causes a reduction of the dielectric constant, creates a higher loss tangent, and shows a significant relaxation process of PU as a thermoplastic part. This result implies that adding more polyurethane content into the system decreases the electronic polarizability due to the lower polarizability of the bulky urethane group at high frequency. The higher polyurethane content leads to diminished molecular packing efficiency and also increases the free volume due to the existence of dissimilar chains. Therefore, more air could be trapped in the polymer chain, resulting in obtaining poor dielectric properties. The presence of air in the specimens was further evaluated through density measurement. Besides, the study on thermal properties of copolymers cloud assess the synergism of two components because inappropriate of urethane adding would have an impact on degradation of materials as a result of less thermally stable of urethane.

4.4.1.5 Density measurement

With respect to the parent resins, the densities of the pure aniline-based polybenzoxzine and polyurethane are 1.196 g/cm^3 and 1.05 g/cm^3, respectively. To observe the presence of void in the specimens, the analytical balance with density kit according to ASTM D 792-00 was performed as relative density measurement. The process was followed 4.3.5. and then three times of the analysis were averaged. Additionally, the density of the samples can be calculated by the basic equation illustrated below [19].

$$\text{Density} = \left(\frac{a}{b-c}\right) * D_{\text{water}} \qquad (4.1)$$

Where: a = weight of the sample in air

b = weight of the sample immersed in deionized water

c = weight of the damp sample after being wiped off excess water

D_{water} = density of deionized water

For the basic of measurement, theoretical density of prepared materials was calculated by using equation (4.2) as followed:

$$\rho_T = (1 - \emptyset)\rho_1 + \emptyset\rho_2 \qquad (4.2)$$

Where ρ_1 is the density of polyurethane, ρ_2 is the density of polybenzoxazine and $\emptyset$ is the volume fraction of polybenzoxazine. The relative density of the cured BA-a/PU at 90/10, 80/20, 70/30, 60/40, and 50/50 was compared with theoretical density calculated from the true density of the starting materials as summarized in Table 4.1 and Fig. 4.10, respectively. The density indicates that the drop in the dielectric constant could be attributed to the existence of porosity in the copolymers due to the low relative permittivity value of the air (dielectric constant of air is 1), which has a severe consequence on the dielectric constant. Subsequently, higher defects such as voids and porosity are inclined to increase loss tangent as well [20, 26].

Table 4.1 The density of BA-a/PU alloys at different urethane contents

BA-a/PU (vol.%)	Density (g/cm^3)	
	Relative	**Theoretical**
90/10	1.172	1.181
80/20	1.151	1.167
70/30	1.148	1.152
60/40	1.130	1.138
50/50	1.108	1.123

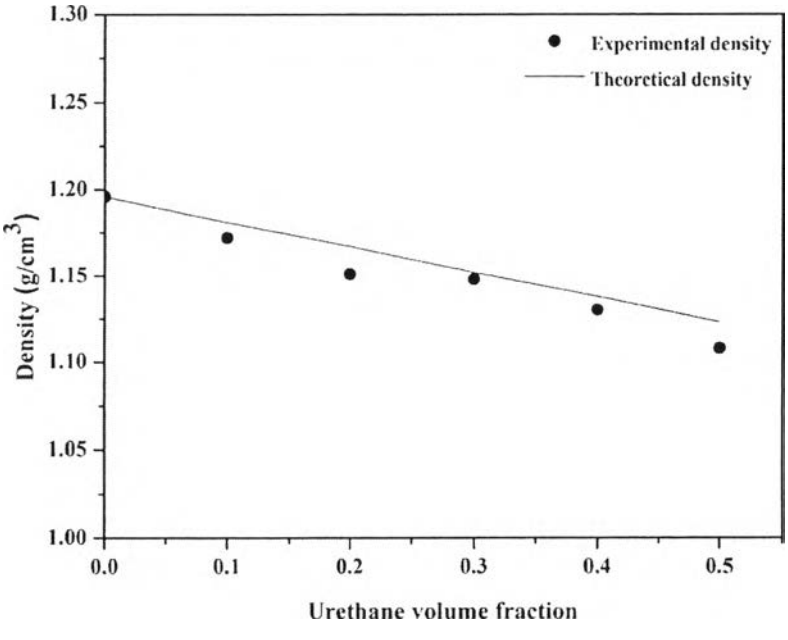

Figure 4.10 Density of poly(benzoxazine/urethane) copolymers at various volume fractions of urethane: (•) experimental and (-) theoretical density.

4.4.1.6 Thermal Gravimetric Analysis (TGA)

The thermal stability of cured poly(BA-a) and BA-a/PU alloys was investigated using TGA. The results are summarized in Table 4.2, and typical TGA thermogram is shown in Fig. 4.11.

It is observed that the degradation temperature (T_d), at 5 and 10% weight loss of binary mixtures shows higher thermal stability than the neat polyurethane. This characteristic derives from aromatic polybenzoxazine, which are more thermally stable and less incline to decompose. However, the advantage of adding urethane content is still appeared. The prepared alloys at 10, 20, and 30 vol.% of urethane portions cloud enhance T_{d5} value to higher than those of the parent polymers. In contrast with larger urethane volume fraction (40 and 50 vol.%), the T_{d5} is likely to decrease. Nevertheless, T_{d10} of the binary system exhibits high thermal stability. The rapid decomposition is found at the initial step on account of the excessive part of urethane resin, which cannot participate in the reaction. This result conforms to the investigation of the curing exotherms by DSC. Furthermore, the char yield, i.e., the residual weight was noted at 900 °C. It is evident from Table 4.2 that the char yield of copolymers is prone to be decreased with the increasing urethane prepolymer fraction. This reduction results from a less thermally stable of aliphatic structure of polyurethane compared with the more stable benzene rings in the structure of polybenzoxazine, which the decomposition is initiated at the urethane linkage. Therefore, the addition of only small amount of urethane prepolymer is suggested for obtaining the superior thermal stability. This added is also appropriate for improving the dielectric properties corresponding to the dielectric study as discussed earlier [21-22].

Table 4.2 Thermal properties of (BA-a/PU)/BST composites

BA-a/PU (vol.%)	T_{d5} (°C)	T_{d10} (°C)	Residual weight (%) at 900°C
100/0	314.0	337.6	27.4
90/10	322.6	345.3	28.2
80/20	327.6	348.2	27.7
70/30	321.2	348.1	25.7
60/40	287.5	347.1	22.9
50/50	278.3	346.6	19.6
0/100	280.1	306.6	1.7

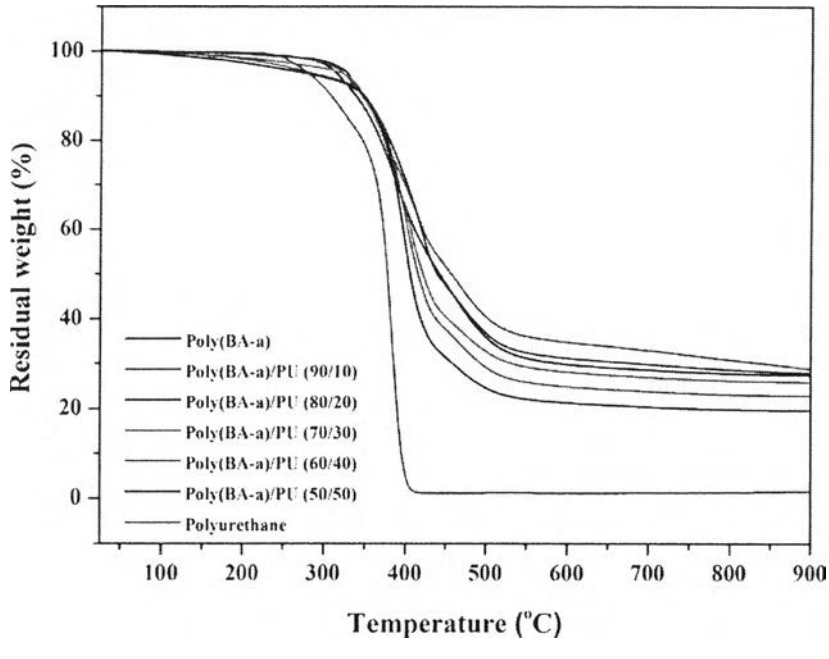

Figure 4.11 TGA thermogram of cured BA-a/PU at various compositions

4.4.1.7 Atomic force microscopy (AFM) Analysis

Atomic force microscopy (AFM) experiments were performed by force modulation mode (FMM) at ambient temperature in air. Since the use of SEM technique was failed to perceive the appearance of phase separation for this system. Using FM-mode is therefore one of preference ways to observe the dispersion of

urethane resin in benzoxazine matrix by observing the relationship of acquired force at various points.

The surface morphologies and mechanical properties in microscopic level of cured BA-a/PU at 100/0, 90/10, 80/20, and 50/50 were examined as displayed in Fig. 4.12 and Table 4.3, respectively. It is clear, by comparing the images (a)-(d) and mechanical properties in microscopic scale, at 50/50 vol.% of the cured BA-a/PU creates more wrinkled surface and larger deviation in hardness and Young's modulus than the system with lower benzoxazine ratio. This phenomenon may result from the overabundance of massive urethane, causing improper interaction between hard segments of aromatic polybenzoxazine and soft segment of polyurethane. This 50/50 vol.% results could refer to the presence of microphase-separated morphologies. On the other hand, the narrow gap in hardness and Young's modulus of the cured BA-a/PU at 90/10 and 80/20 vol.% was found. These obtained variation values are very close to the pure system, which indicates the highly compatible copolymer. Another observation, the hardness of the mixtures tends to be decrease with the higher amount of urethane content. Similar to Young's modulus, the reduction in its values are gained by adding urethane in the system. This can conclude that the binary system shows higher flexibility than the neat BA-a due to the presence of soft segment-rich domains of elastic urethane, which is attributed to the high aliphatic content in the system. This experiment is in agreement with the previous studies made by DSC, TGA, and dielectric study, suggesting that the several outstanding properties are achieved with the combination of small amount of polyurethane.

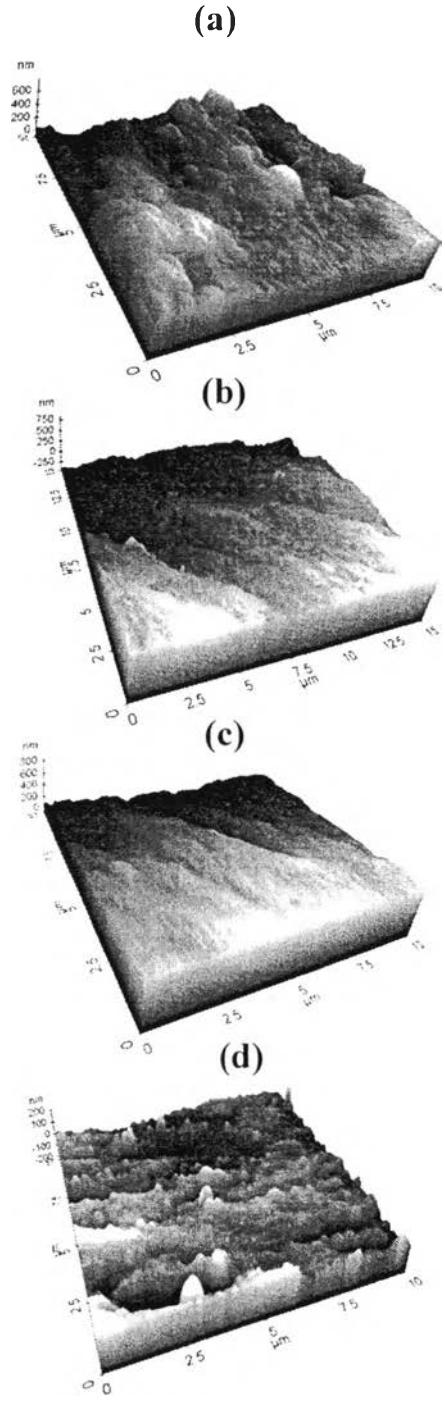

Figure 4.12 AFM morphology of cured BA-a/PU alloys: (a) 100/0, (b) 90/10, (c) 80/20, (d) 50/50 : topographic images.

Table 4.3 The mechanical properties in microscopic level of cured BA-a/PU at 100/0, 90/10, 80/20, and 50/50 vol.% monitored by AFM in FM-mode

Materials	Hardness (Pa)	Young's modulus (kPa)
BA-a	891 ± 6	176 ± 7
BA-a/PU(90/10)	799 ± 20	150 ± 4
BA-a/PU(80/20)	724 ± 14	147 ± 3
BA-a/PU(50/50)	739 ± 55	146 ± 14

4.4.1.8 Dynamic Mechanical Analysis (DMA)

With respect to the aforementioned characterizations of the binary mixtures between BA-a and PU at various compositions, it is found that the incorporation of small amount of PU yields numerous outstanding characteristics with no phase separation noticed after observed by AFM. Apparently, the superior dielectric properties, which are an important factor of this research were obtained at 90/10 vol.% of BA-a/PU. Hence this fraction was used as a polymer matrix for composite fabrication.

To investigate the glass transition temperature of the polymer based used, DMA technique was performed owing to its performance to detect even minor change in molecular relaxation [13]. The broad temperature range by scanning from -100 °C to 250 °C was measured, which is covering the glass transition region of original resins in order to identify the compatibility of the mixture. The dynamic mechanical properties of the pure BA-a and BA-a/PU (90/10 vol.%) are exhibited in Figure 4.13.

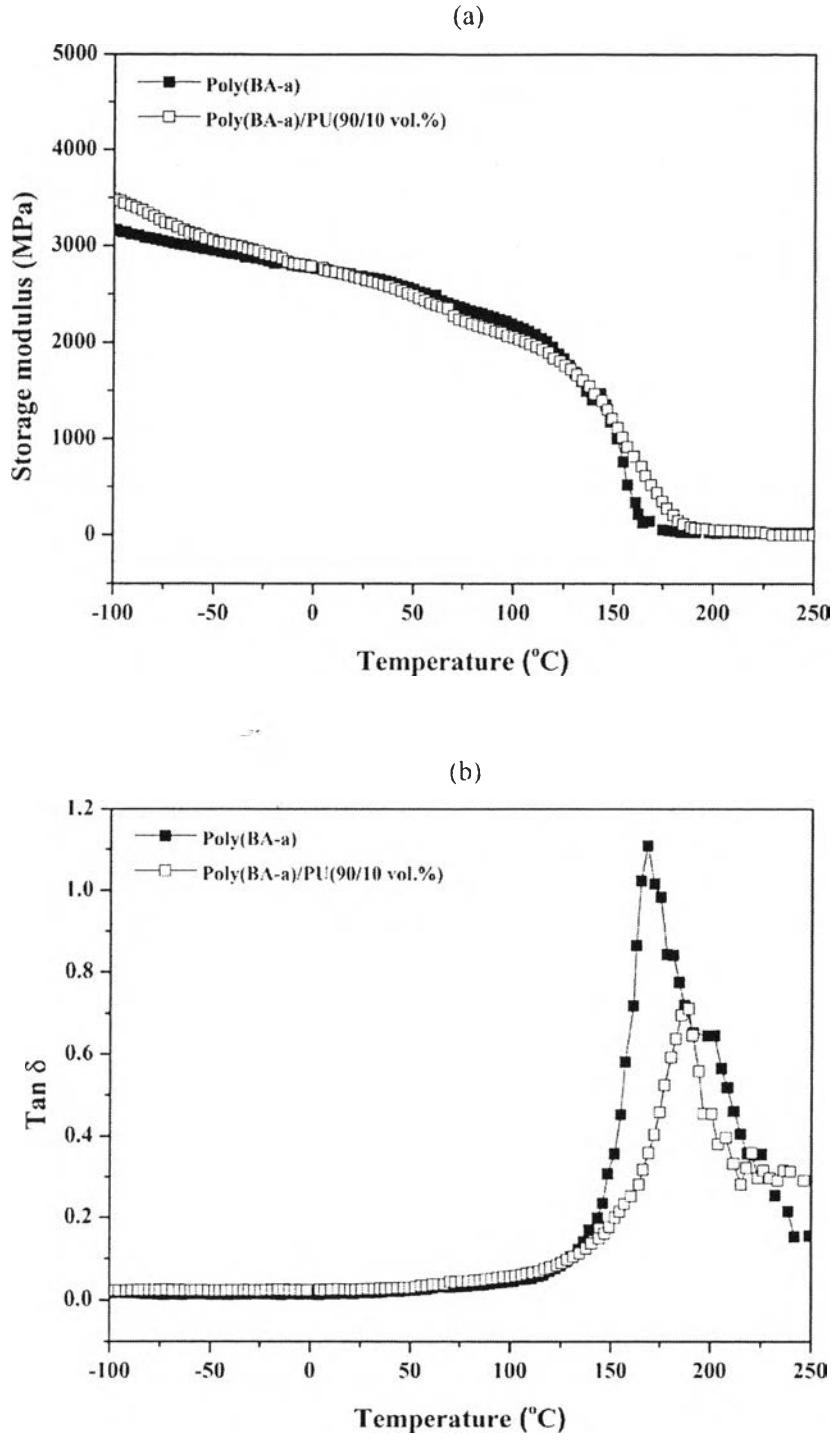

Figure 4.13 DMA thermograms of the neat BA-a and BA-a/PU (90/10 vol.%) : a) storage modulus and b) Loss tangent (tan δ).

The DMA thermogram shows that at very low temperature, the initial storage modulus (E') of the BA-a/PU (90/10 vol.%) is higher than the neat BA-a.

Then the modulus of the mixture system gradually decreases when the temperature ramps up and again increases beyond the modulus of BA-a in the rubbery state. According to the T_{gs} of the PU and BA-a were reported by Rimdusit group to be about –70 °C and 165°C, respectively. For this experiment, T_{gs} of samples were defined using the maximum of the tan δ. It is found that T_g of BA-a is 168 °C. For the binary system, T_g of 90/10 vol.% of BA-a/PU is 189 °C, which is evidently greater than the parent polymers. The higher glass transition and higher storage modulus at initial and in rubbery states of BA-a/PU probably derived from the intermolecular hydrogen bonding type by interactions between urethane clusters and phenolic and Mannich amine bridges of the polybenzoxazine unit. This phenomenon can be supported by the shift of some absorption peaks in the FTIR spectra of binary systems in comparison to the pure component. Still, this explanation can be strongly supported by Jamshidi report that the presence of urethane groups is strong tendency for hydrogen bonding interactions (as both donor and acceptor) [22]. On the other hand, the lowering of modulus at higher temperature is also found with the presence of the PU in the binary mixture. This is because the more flexible characteristics and greater degree of molecular mobility of the PU elastomer. The PU molecule contains numerous ether linkages in which the internal movement of the molecules is very active compared with the rigid phenolic structure of the polybenzoxazine; thus, conducing to the lowering of the stiffness of the alloys [21]. Additionally, at 90/10 vol.% of BA-a/PU shows single tan δ peak. This observed synergistic behavior can suggest that no macroscopic phase separation indicating a potential use for matrix of the composites.

4.4.2 Barium Strontium Titanate ($Ba_{0.3}Sr_{0.7}TiO_3$) Characterizations

4.4.2.1 X-Ray Diffraction (XRD) Analysis

In this work, X-ray diffraction measurement was carried out to examine the crystallization of the present material, barium strontium titanate (BST), prepared via sol-gel method. The XRD pattern of ceramic fillers after the calcinations process is seen in Figure 4.14. It indicates the reflection peaks at 2θ values of 22.6°, 32.2°, 39.6 °, 46.1 °, 51.9 °, 57.4 ° and 67.3 ° corresponding to (100), (110), (111), (200), (210), (211) and (220) set of diffraction planes, respectively. These reflection results refer to the perovskite structure. Besides, the cubic structure of BST particles can be confirmed by the absence of peak splitting at 2θ =46.1°. From the XRD pattern, the weak peak of undesirable phase is also found, which is assigned to those of alkaline earth carbonate ((Ba,Sr)CO_3) [23].

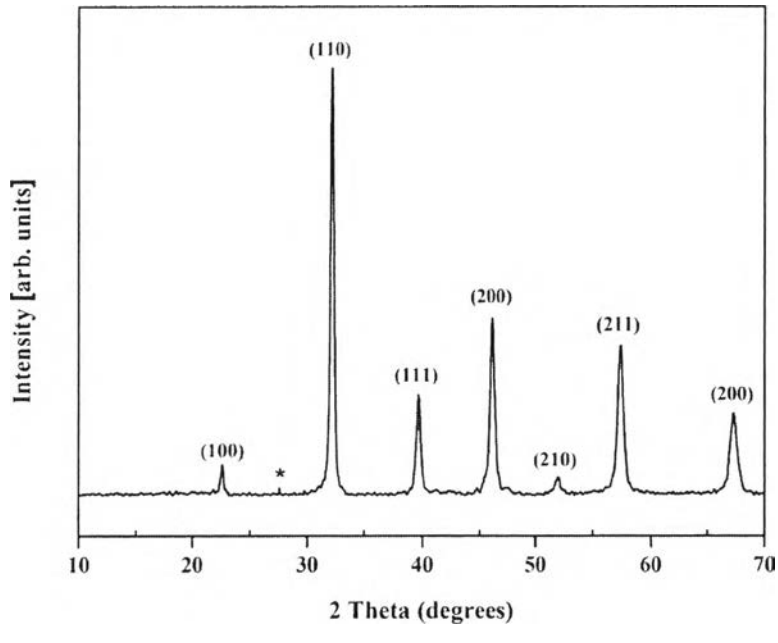

Figure 4.14 The X-ray diffraction pattern of BST ceramic fillers prepared via sol-gel method.

4.4.2.2 Fourier Transform Infrared Spectroscopy (FTIR) Analysis

To confirm functional groups of BST powder, FTIR measurement was introduced as shown in Fig 4.15. The observed absorption band at 561 cm^{-1} indicates the Ti-O stretching vibration of a TiO_6 octahedron. Another band is located at 1432 cm^{-1}, which corresponds to C=O stretching of carbonate ion impurities in BST fillers [24].

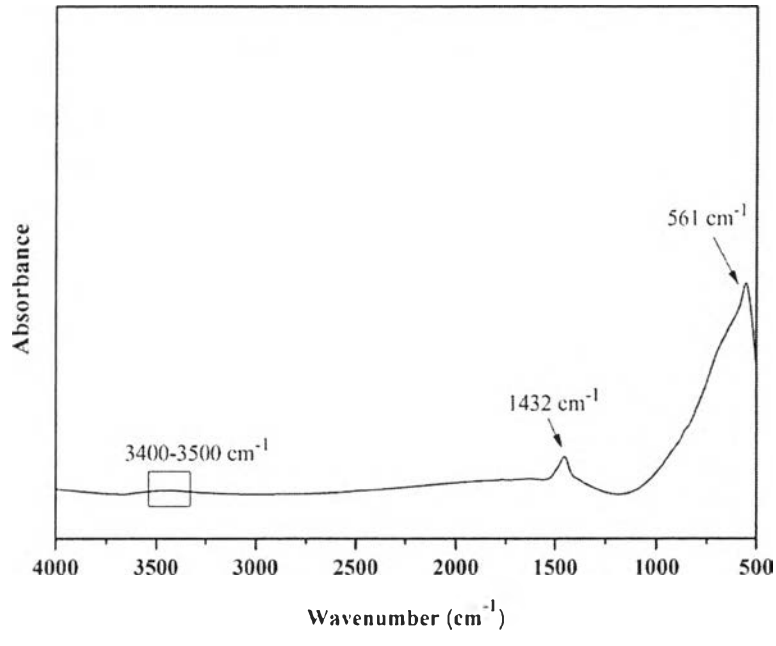

Figure 4.15 The FTIR spectrum of BST ceramic fillers prepared via sol-gel method.

4.4.2.2 Transmission Electron Microscopy (TEM) and Scanning Electron Microscopy (SEM) Analysis

TEM and SEM techniques were used to observe the morphology of the BST powder prepared via sol-gel method. TEM and SEM images are shown in Fig. 4.16 and 4.17, respectively.

As appeared in TEM and SEM images, the particles are mostly agglomerate and uniformly particles size with shape distribution. According to this measurement, the average diameter of crystallites is found to be 40–80 nanometers for $Ba_{0.3}Sr_{0.7}TiO_3$.

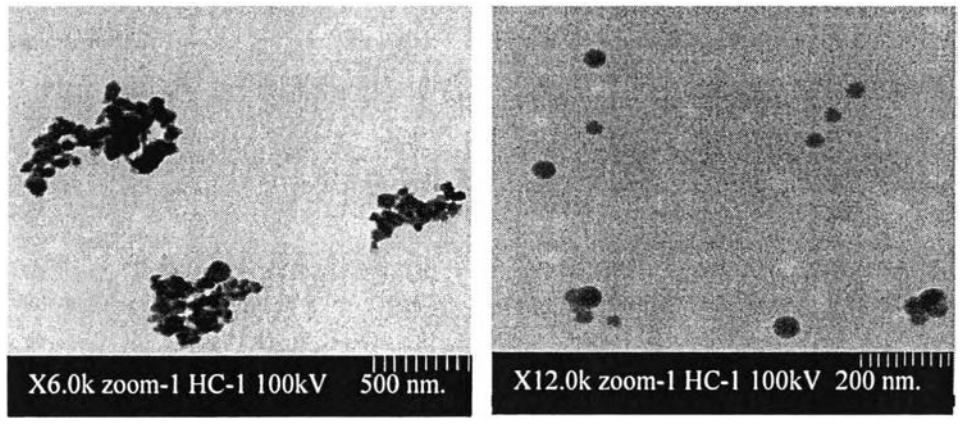

Figure 4.16 TEM image of BST powder prepared by sol-gel method.

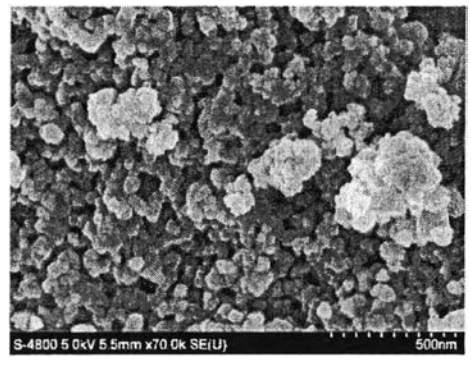

Figure 4.17 SEM image of BST powder prepared via sol-gel method.

4.4.3 Poly(benzoxazine/urethane)/Barium Strontium Titanate Composites Characterizations

4.4.3.1 Microwave Dielectric Properties Measurements

Regarding to the study of dielectric behaviors of poly(benzoxazine/urethane) copolymers, (BA-a/PU), the suitability of polymer matrix is at 90/10 vol.% of BA-a/PU. Thus this composition was used as a polymer matrix for fabricating the composites. In the part of ceramic filler, barium strontium titanate ($Ba_{0.3}Sr_{0.7}TiO_3$) was introduced into the polymer matrix owing to their high permittivity with low loss tangent at high frequency [25]. The composite materials were prepared via the melt mixing process by varying BST content from 30 wt.% to 60 wt.%. The dielectric characteristics of the composites were studied in the frequency range of 300 MHz to 1 GHz with the temperature variation from -50 °C to

150 °C. The temperature dependence of the permittivity and dissipation factor of composites with various BST loadings is shown in Figure 4.18a and b, respectively.

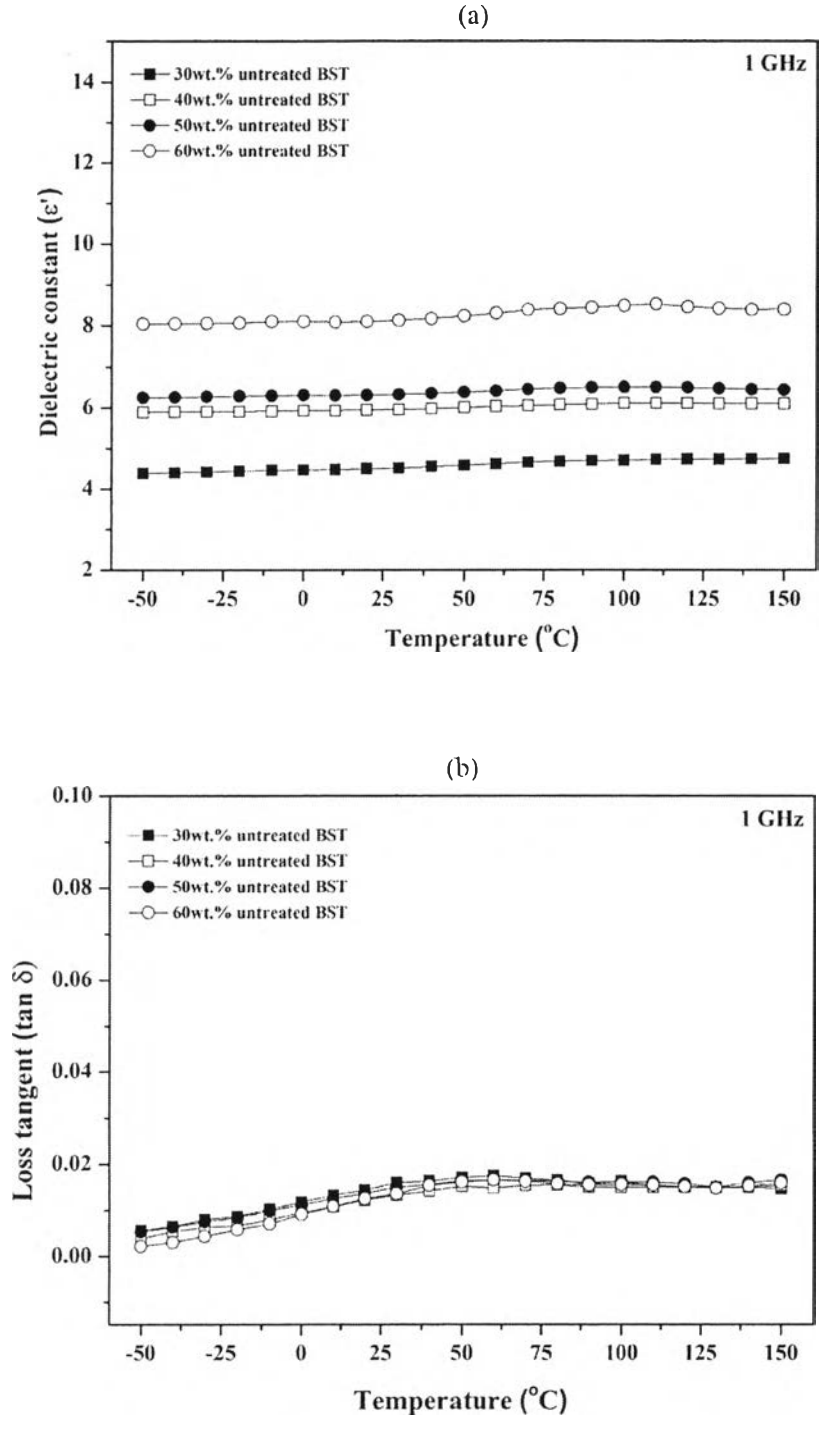

Figure 4.18 Temperature dependence of a) dielectric constant and b) loss tangent of BA-a/PU composites by varying BST contents measured at 1 GHz.

It can be seen in Fig. 4.18a, that at various temperatures (1 GHz), the dielectric constants of the composites increases in relation to the amount of BST powders. A higher ceramic filler loading, the ceramic particles enable to come closer, leading to an increased dipole-dipole interaction, contributing to a higher dielectric constant [26]. Furthermore, the relative permittivity of all components in the presence of BST is usually stable under different temperature circumstances. This superior property could have originated from the synergism between the polymer and ceramic phases. Therefore, the rigidity of the ceramic filler could help diminish the relaxation process of the polymer matrix. In contrast, the effect of ceramic particles addition has less impact on loss tangent as displayed in Fig 4.18b. The temperature has a small influence on this factor because the loss is not only dependent on the material, matrix, and fillers, but also on the interconnectivity, or phase properties, geometry of the dispersed phase (particles size, distribution, orientation) [27]. Nonetheless, the dissipation factor of all composites is still less than 0.0175 with identical inclination pattern forms.

Even though above 60 wt.%, the BST loading could substantially enhance the dielectric constant, the material has poor mechanical properties. Therefore, in this research, the amount of BST loading is limited to 60 wt.%.

In addition, the study of frequency dependence is one of the most significant factors for indicating the performance of the composites when they were operated. The dielectric behaviors of four composites under varying BST weight fractions (30, 40, 50, and 60 wt.%) measured at room temperature in the frequency range of 300 MHz to 1 GHz as seen in Fig. 4.19a and b.

(a)

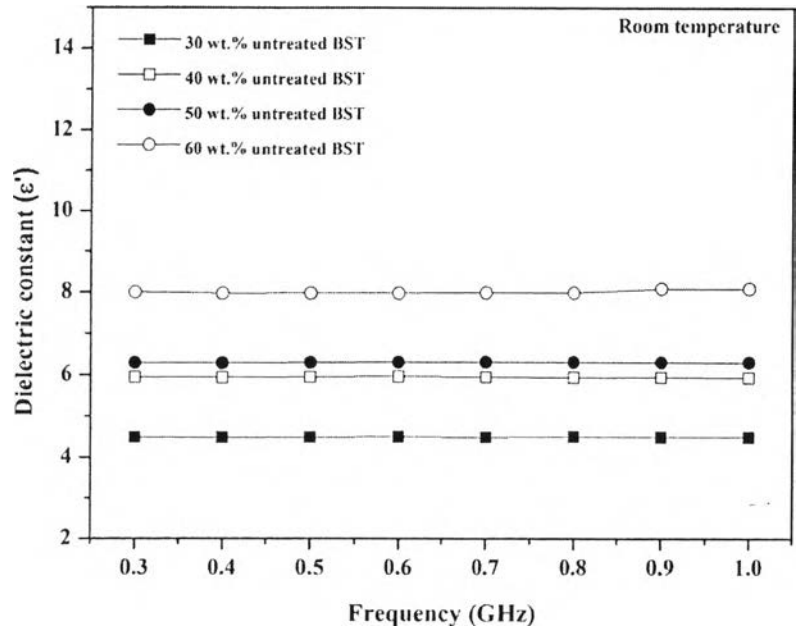

(b)

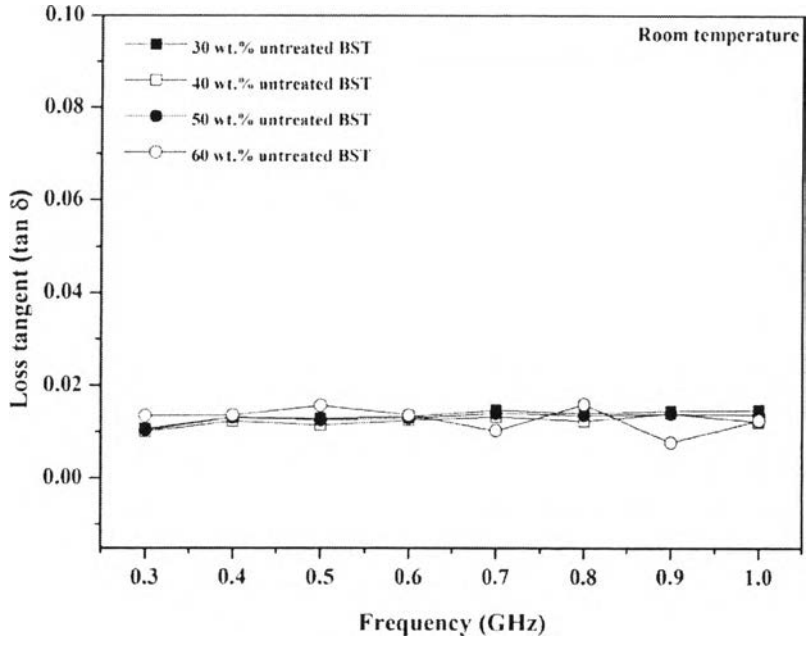

Figure 4.19 Frequency dependence of a) dielectric constant and b) loss tangent of BA-a/PU composites by varying BST contents measured at room temperature.

The dielectric constant of the composite shifts from 4.49 to 8.10 at 30 wt.% and at 60 wt.% of BST loading, respectively. The relative permittivity and dissipation factor of prepared composites exhibit nearly identical linear dependence at observed frequency range, which refers to the frequency independence characteristic (Fig. 4.19a). A small scattering of the dielectric constant is only found at 900 MHz of 60 wt.% of BST content. Furthermore, the values of dielectric loss tangent for the composites loaded with 30 wt.% and 60 wt.% are 0.015 and 0.0125, respectively. These factors can meet the required properties (<0.03) as shown in Fig. 4.19b. This implies that the composites are applicable for high frequency applications (300 MHz - 1 GHz).

4.4.3.2 Thermal Gravimetric Analysis (TGA)

Figure 4.20 depicts the thermogravimetric analysis (TGA) thermograms of BA-a/PU composites at various BST contents under nitrogen atmosphere and the specific thermal data is summarized in Table 4.4. To examine thermal stability of the composites, degradation temperature (T_d), was reported at 5% and 10% weight losses with the residual weight at 900 °C. Clearly, the thermal stability of the composites is significantly enhanced with higher amount of BST. By adding 60 wt.% of BST, the degradation temperature (T_{d5}) of the materials was shifted from 322.6 to 371.4. The results could be confirmed that the present of BST is in good entanglement with the polymer matrix resulting in the movement of the polymer phase is limited. As a consequence, the interconnection between two phases is improved, which is able to retard the degradation of the composites by shifting decomposition temperature to higher values. In the same way, a direct indication of resistance to combustion—char yield of the composite systems is found to enhance steadily with increasing the mass fraction of the BST because the nature of BST structure is thermally stable up to very high temperatures. As can be seen in Table 4.4, 28.2 % of the residual weight of the neat poly(BA-a)/PU is uplifted to 74.2 after adding 60 wt.% of BST. It is confirmed that the existence of higher amount of BST improves not only the dielectric properties as former mention but also thermal properties [28-29].

Table 4.4 Thermal properties of BA-a/PU composites at various compositions with 30, 40, 50, and 60 wt.% of BST loading

[BA-a/PU(90/10 vol.%)]/BST (wt.%)	BST Volume fraction	T_{d5} (°C)	T_{d10} (°C)	Residual weight(%) at 900°C
100/0	0	322.6	345.3	28.2
70/30	0.0918	335.1	358.4	51.7
60/40	0.1387	340.0	371.4	60.0
50/50	0.1987	364.9	377.2	66.4
40/60	0.2614	371.4	399.3	74.2

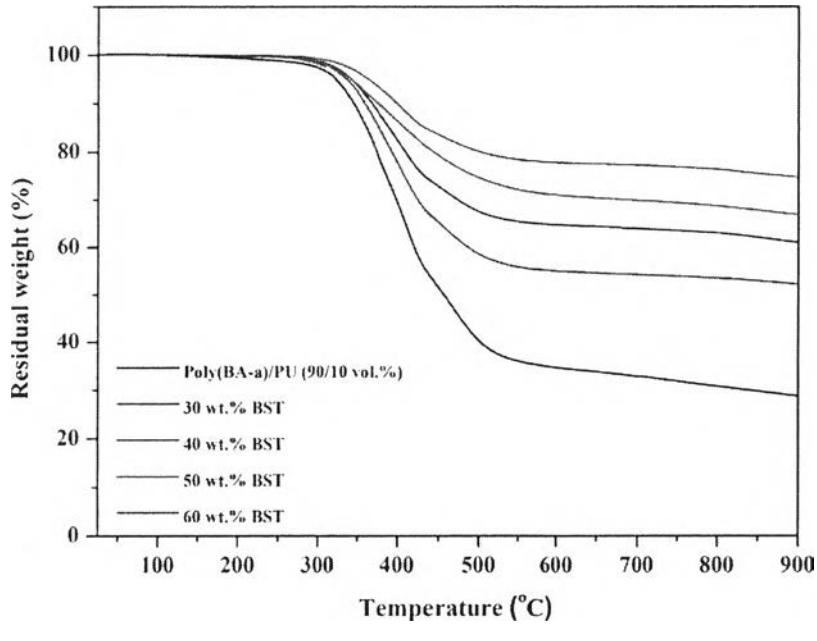

Figure 4.20 TGA thermogram of BA-a/PU composites at various compositions with 30, 40, 50, and 60 wt.% of BST loading.

4.4.3.3 Dynamic Mechanical Analysis (DMA)

The dynamic mechanical curves shows the temperature dependence of the storage modulus (E') and loss factor (tan δ) of BA-a/PU composites by varying BST contents at 30, 40, 50, and 60 wt.% as depicted in Figures 4.21 (a, b).

As a measurement of material stiffness under shear deformation can be observed from the initial storage modulus E' of a solid specimen at ambient temperature, the stiffer material would have higher storage modulus at initial. It is evidently from Fig. 4.21a that BA-a/PU composites have higher storage modulus over the entire temperature range than the pure BA-a/PU polymer matrix and this parameter is increased by adding higher amount of BST nanofiller. The initial storage modulus of the composite is increased from 3.5 to 7.7 GPa at 60 wt.% of BST. This enhancement is supported by the substantial nanoreinforcement of BST to the system. Moreover, the glass transition temperature (T_g) notices at the maximum tan δ is found to be increased from 189.0 °C to 222.7 °C with the amount of BST loaded in the polymer matrix (0 to 60 wt.% of BST). This change has been strongly attributed to restricting the segmental motion of the polymer chains by the rigidity of BST nanoparticle. This constraint in turn creates a change in the density of the polymer chain packing in the neighborhood of the BST gain, leading to the modification of the conformation and orientation of chain segments. Therefore, the higher temperatures are essential for pulsing chains pass together, which is the point to indicate glass transition temperature [28-30].

(a)

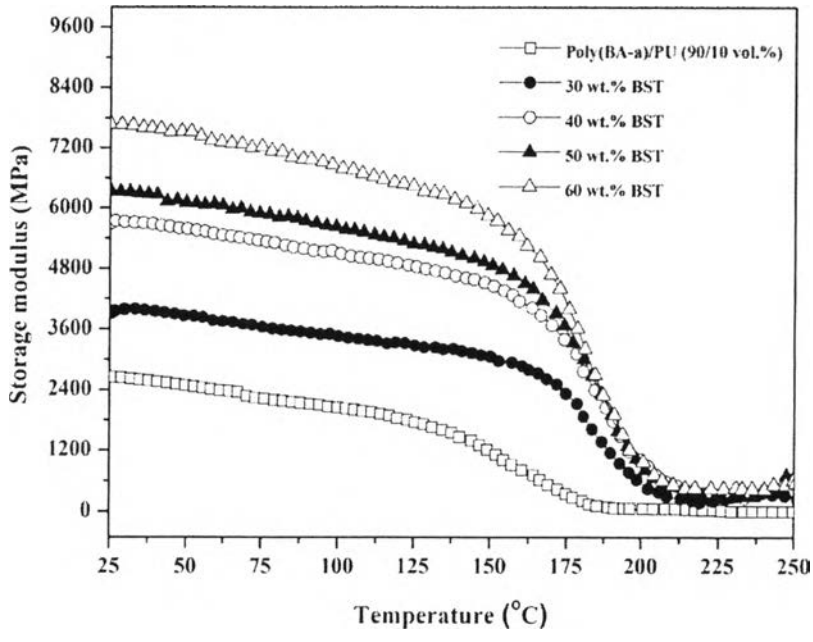

(b)

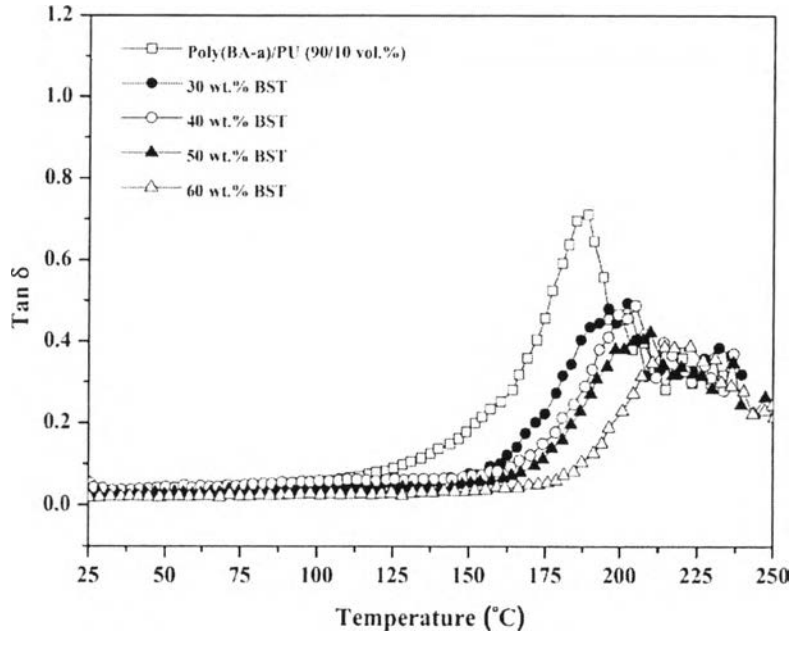

Figure 4.21 DMA thermograms of a) storage modulus and b) tan δ of BA-a/PU composites by varying BST loadings.

4.4.3.4 Atomic force microscopy (AFM) Analysis

The mechanical characteristics evaluated by atomic force microscopy (AFM) analysis in force modulation mode (FMM) for measurement provides more quantitative characterization of polymer composite behaviors under mechanical loads. According to FMM operation, the mechanical data including Young's modulus and hardness are presented in Table 4.5. It is found that the BA-a/PU composites exhibit higher Young's modulus and hardness compared to the neat polymer based, which is in agreement to dynamic mechanical analysis. The hardness of adding 60 wt.% of BST in the polymer matrix dramatically shifts from 0.80 to 2.78 kPa. In the same manner, the modulus value is also increased from 150.08 to 187.50 kPa. These phenomena are derived from the higher stiffness of BST filler. Nevertheless, at different BST contents do not largely affect to those values owing to the identical embedded characteristic of BST in polymer matrix and also the determination of mechanically microscopic level.

Table 4.5 The mechanical properties in microscopic level of BA-a/PU composites at various BST contents monitored by AMF in FM-mode

[BA-a/PU(90/10 vol.%)]/BST (wt.%)	**Hardness (kPa)**	**Young's modulus (kPa)**
100/0	0.80 ± 0.02	150 ± 4
70/30	2.64 ± 0.12	182 ± 3
60/40	2.57 ± 0.13	177 ± 5
50/50	2.38 ± 0.04	181 ± 12
40/60	2.78 ± 0.14	187 ± 6

4.4.3.5 Density Measurement

The densities of BA-a/PU composites at various BST contents were performed to observe the existence of porosity in the specimens as followed ASTM D 792-00. Theoretical density of material was also calculated by using equation (4.3) as shown below:

$$\rho_T = (1 - \emptyset)\rho_p + \emptyset\rho_c \quad (4.3)$$

Where ρ_c is the density of ceramic filler, ρ_p is the density of polymer matrix and $\emptyset$ is the volume fraction of ceramic filler. The calculation was based on the densities of the neat 90/10 (vol.%) of BA-a/PU as polymer matrix and BST particles, which are 1.179 and 5.412 g/cm^3, respectively. Table 4.6 summarizes the densities of the BA-a/PU composites at various BST contents. The experimental density can fit well with the theoretical density at small amount of BST loading. For higher BST content, the obtained density is slightly lower than the theoretical density as illustrated in Fig. 4.22. This experimental density deviation is prone to be caused by the presence voids in the samples on account of the difficulty in mixing at large amount of BST.

Table 4.6 Density of the composite at various contents

[BA-a/PU(90/10 vol.%)]/BST (wt.%)	Volume fraction	Density (g/cm^3)	
		Relative	Theoretical
70/30	0.0918	1.554	1.568
60/40	0.1359	1.738	1.754
50/50	0.1908	1.896	1.987
40/60	0.2614	2.016	2.286

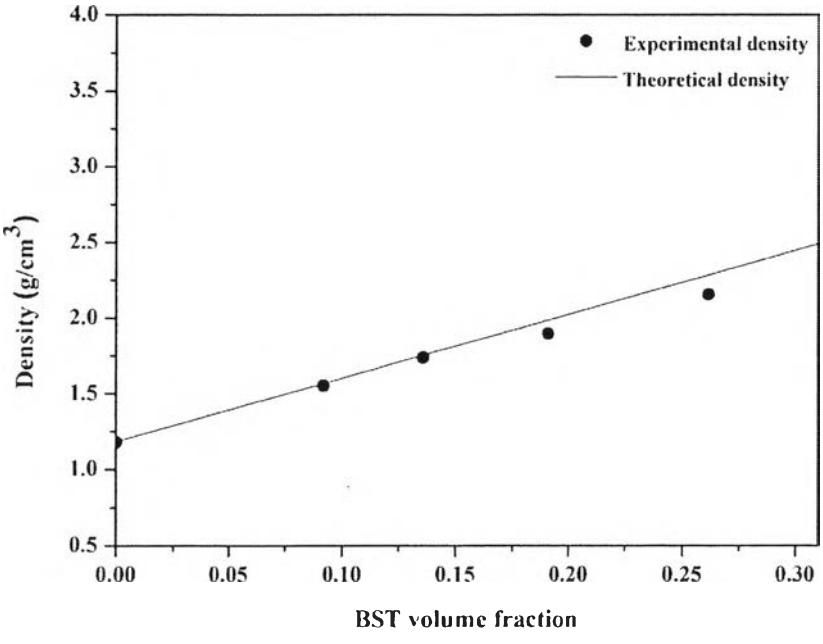

Figure 4.22 The comparison between (•) experimental and (-) theoretical density as a function of BST volume fraction.

4.4.3.6 Scanning Electron Microscopy (SEM) Analysis

For fabricating polymer/ceramic dielectric materials with good dielectric characteristics, the dispersion of fillers is extremely vital. Thus the morphological observation using SEM technique is required. In this work, the surface morphology of BA-a/PU composites at of 30, 40, 50, and 60 wt.%, of BST loading was observed as shown in Figure 4.23 (a)-(d). The white and back colors indicate the part of BST filler and the polymer matrix, respectively. As can be seen in SEM images, the distribution of BST powder is not uniformly dispersed. Although at the lowest BST content (30 wt.%) was added, the BST filler is likely to agglomerate. The forming of large cluster is induced by the high surface energy of BST nanoparticle. This agglomeration of ceramic filler needs to improve further by modifying surface of nanoparticle in order to acquire the superior dielectric properties [9, 31-32].

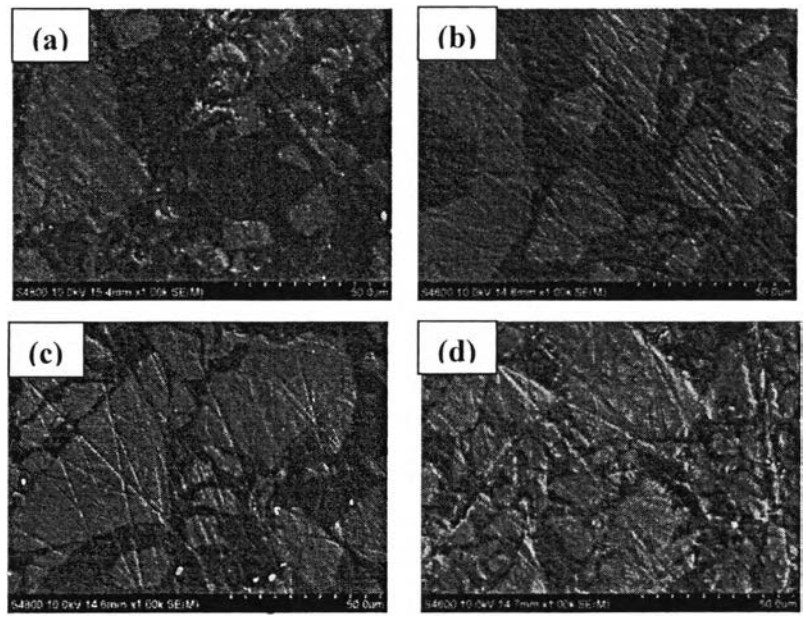

Figure 4.23 SEM images of the surface morphology of BA-a/PU composites at various BST loading (a) 30 wt.% (b) 40 wt.% (c) 50 wt.% (d) 60 wt.%.

4.4.3.7 Experimental Data Fitting

There are several of models have been suggested for the prediction of the relative permittivity of the composites. A variety of formulas derived from the fundamental of various theoretical assumptions and experimental data. Thus in this study, the calculation of four commonly proposed equations in literature was performed and discussed. The models that frequently used are series, Lichtenecker model, Maxwell-Wagner equation and Kerner expression modified by Jayasundere-Smith (J-S prediction). These formulas are described as shown below:

Series model $$\frac{1}{\varepsilon} = \frac{\phi_c}{\varepsilon_c} + \frac{\phi_p}{\varepsilon_p}$$

Lichtenecker model $$\log \varepsilon = \emptyset_p \log \varepsilon_p + \phi_c \log \varepsilon_c$$

Maxwell-Wagner equation $$\varepsilon = \varepsilon_p \frac{2\varepsilon_p + \varepsilon_c + 2\emptyset_c (\varepsilon_c - \varepsilon_p)}{2\varepsilon_p + \varepsilon_c - \emptyset_c (\varepsilon_c - \varepsilon_p)}$$

Kerner expression $$\varepsilon = \frac{\varepsilon_p \phi_p + \varepsilon_c \phi_c [3\varepsilon_p/(\varepsilon_c + 2\varepsilon_p)][1 + 3\phi_c(\varepsilon_c - \varepsilon_p)/(\varepsilon_c + 2\varepsilon_p)]}{\phi_p + \phi_c (3\varepsilon_p)/(\varepsilon_c + 2\varepsilon_p)[1 + 3\phi_c(\varepsilon_c - \varepsilon_p)/(\varepsilon_c + 2\varepsilon_p)]}$$

where ε is the dielectric constant of the composites; ε_p and ε_c refer to the dielectric constants of the polymer matrix and the BST ceramic, respectively; ϕ_c and ϕ_p are the volume fraction of the ceramic and polymer, respectively

Fig. 4.24 shows the dielectric constant of the BA-a/PU composite as a function of volume fraction of BST powder. As anticipated, the relative permittivity of BA-a/PU composite increases with the increasing volume fraction of BST nanofiller. It is found that the value of dielectric constant of the BA-a/PU composites was fitted well with Lichtenecker model at low concentration of BST. Then at higher amount of BST, the dielectric constant of the composites tends to follow Maxwell-Wagner prediction. For predicted the relative permittivity of the composites by those models, it suggested that the composites are a random mixture of nearly spherical inclusions at initial of BST loading. Additionally, at higher concentration of BST, uniformly distributed spherical inclusions of ceramic material with dielectric constant are observed. The deviation is also found from the estimates. This fluctuation may be due to the imperfect dispersion of filler ceramic particle at higher filler contents or due to porosity or air enclosed by the composite, which is detected by SEM and density measurement as mentioned in the previous discussion. It is the fact that the dielectric characteristics of the composites are influenced not only by the dielectric constant of the materials but also by various factors such as the morphology, dispersion, and the interactions between the phases [2, 33].

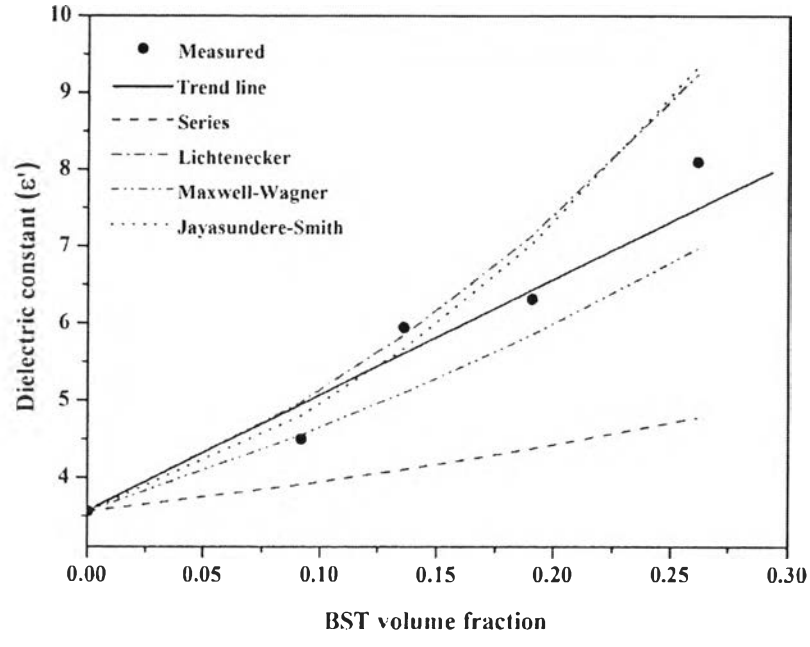

Figure 4.24 Plot of theoretical models and the measured dielectric constant for different BST volume fractions at room temperature and 1 GHz.

4.4.4 Characterization of Poly(benzoxazine/urethane)-Modified BST

4.4.4.1 Fourier Transform Infrared Spectroscopy (FTIR) Analysis

It has been noticed by the various literatures that the outstanding dielectric properties was gained by improving the dispersion of ceramic fillers. A variety of polymer/ceramic composites as dielectric materials has also been prepared with the incorporation of surface modification on filler to enhance the dielectric properties [32-33]. By raising the dielectric capability of BA-a/PU composites, the surface of BST nanoparticle was chemically modified with 3-aminopropyl trimethoxy silane and 5 wt.% of BA-a/PU. The FT-IR spectra of untreated BST particle compared with silane modified BST and 5 wt.% of BA-a/PU treated BST are seen in Fig. 4.25 and 4.26, respectively.

It is found that the system of BST treated with silane coupling agent exhibited different absorption bands around 1021-1129 cm^{-1}. These absorption characteristic are attributed to Si-O-Si unit from the hydrolysis of silane. Also, the weak peak at 1200 cm^{-1} is associated with Si-CH_2 bond. The presence of these characteristic peaks prove that the interaction between surface of BST and silane coupling agent are occurred [3,34].

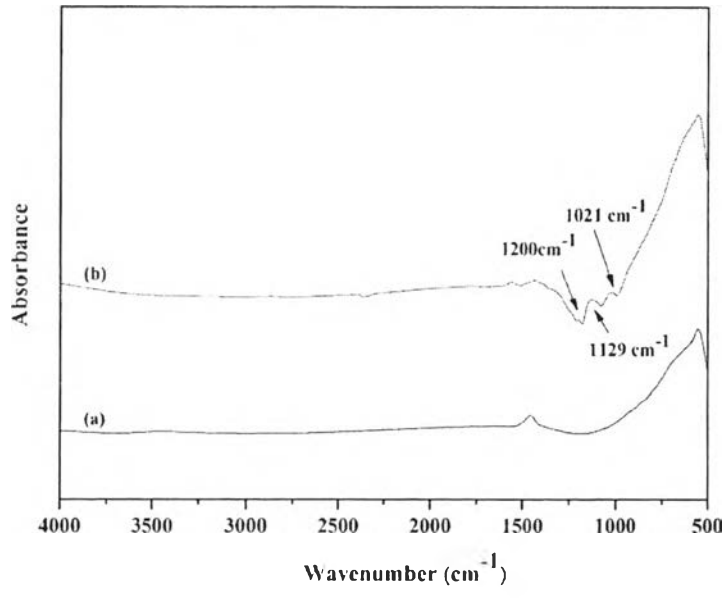

Figure 4.25 The FTIR spectra: (a) BST powder and (b) BST treated with 3-aminopropyl trimethoxy silane.

For the BST coated by 5wt.% of BA-a/PU system, it is evidently from Fig 4.26 that BST powder modified by 5 wt.% of the polymer matrix displays the absorption peak at 1280 cm^{-1} belonging to the asymmetric C-O-C stretching mode. In addition, C-N-C antisymmetric stretching mode presented at 1175 cm^{-1} and 1227 cm^{-1} is found [35].

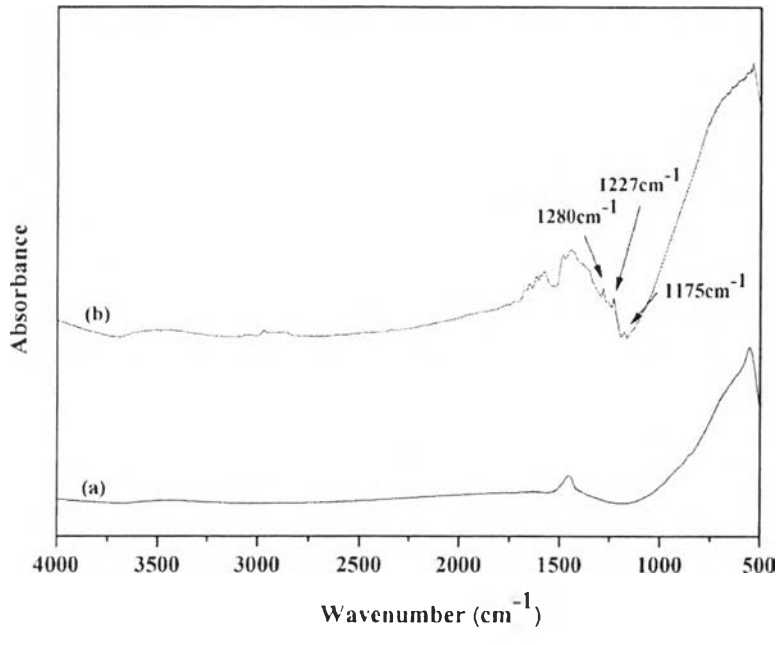

Figure 4.26 The FTIR spectra: (a) BST powder and (b) BST treated with 5 wt.% BA-a/PU.

4.4.4.1 Scanning Electron Microscopy (SEM) Analysis

To investigate the effect of BST surface modification on the distribution of ceramic filler in BA-a/PU matrix, the morphology of the composites was measured by SEM technique.

Figure 4.27 and 4.28 (a)-(c) demonstrate microstructure of the composites at 30 wt.% and 50 wt.% of BST particles which were untreated, treated with silane coupling agent and treated with BA-a/PU, respectively. From the SEM images, it can be seen that the agglomeration of various modified BST methods is improved through out every fraction of BST filler. At different surface modification

routes, it is found that the dispersion of BST by the treatment with BA-a/PU and silane coupling methods is nearly the same. Using BA-a/PU approach takes the advantage from the fact that molecular structure of BA-a/PU is composed of the aromatic rings which are bulky group and the same as polymer matrix. As a consequence, the modified BST with BA-a/PU is impeded to come closer. While the silane coupling agent can form the interlayer between polymer and ceramic. However, some agglomeration of BST is marginally observed due to the large different in density of the two materials [9].

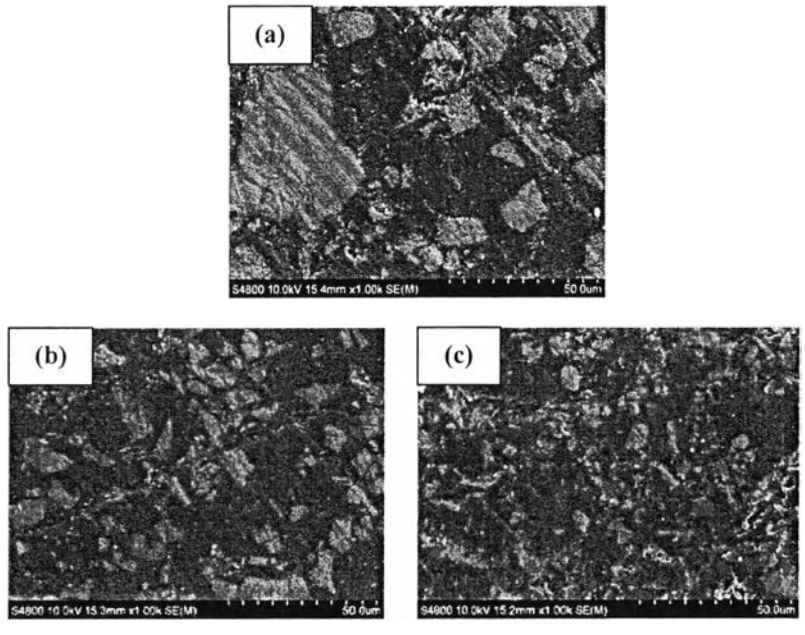

Figure 4.27 SEM micrographs of BA-a/PU composites at 30 wt.% of BST with (a) untreated BST powder, (b) silane treated BST powder, and (c) BA-a/PU treated BST powder.

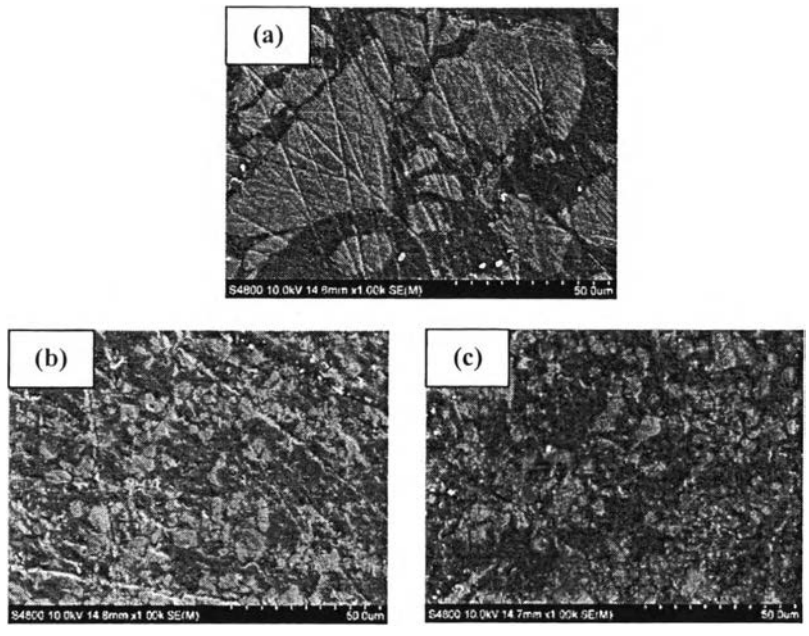

Figure 4.28 SEM micrographs of BA-a/PU composites at 50 wt.% of BST with (a) untreated BST powder, (b) silane treated BST powder, and (c) BA-a/PU treated BST powder.

4.4.4.1 Microwave Dielectric Properties Measurements

The dielectric characteristics including the relative permittivity and loss tangent between untreated BST, BST modified by BA-a/PU, and BST modified by silane coupling were compared. The temperature dependence ranging from -50 °C to 150 °C was studied at 30, 40, 50, and 60 wt.% as shown in Fig. 4.29-4.32, respectively. The study under frequency dependence in the range of 300 MHz to 1 GHz was also performed at the same composition as presented in Fig.4.33-4.36, respectively. It is clear that the highest dielectric constant at every BST fraction with various atmospheres is derived from the introducing of surface modification by silane coupling agent. For BA-a/PU treatment, the dielectric constant is also improved from the untreated system. The large improvement in dielectric constant is found as a result of the forming of chemical bonds on the surface of BST can increase the adhesion between two phases, which results in obtaining higher polarizability. For the loss tangent, the systems of surface treatments and untreated are nearly the same. The dissipation factor of entire compositions is found to be

lower than 0.03. As observed the dielectric properties under temperature and frequency dependence, poly(benzoxazine/urethane) combines with barium strontium titanate exhibite the exceptional dielectric characteristics with mostly stable at different atmospheres.

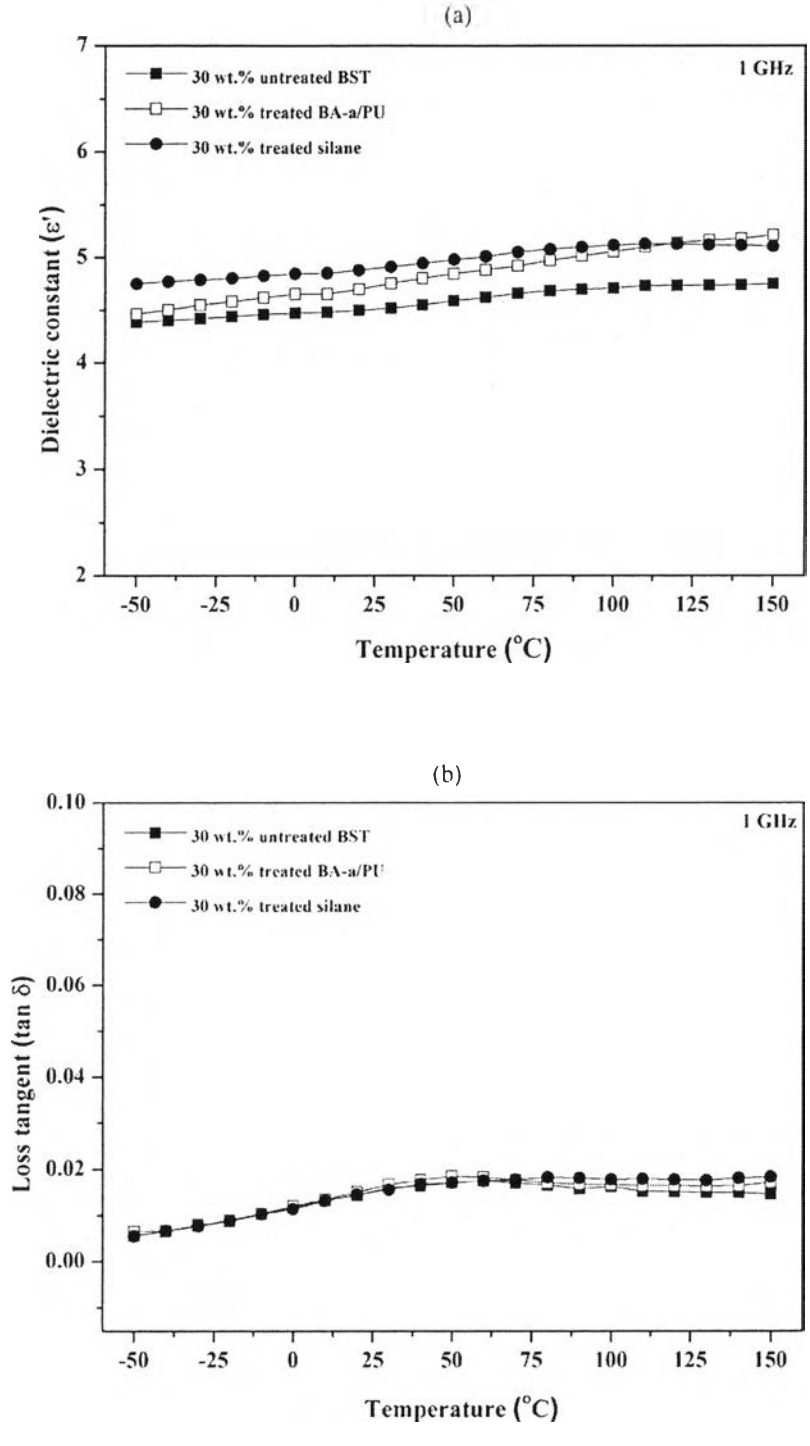

Figure 4.29 Temperature dependence of a) dielectric constant and b) loss tangent of poly(benzoxazine/urethane) composite at 30 wt.% of BST measured at 1 GHz.

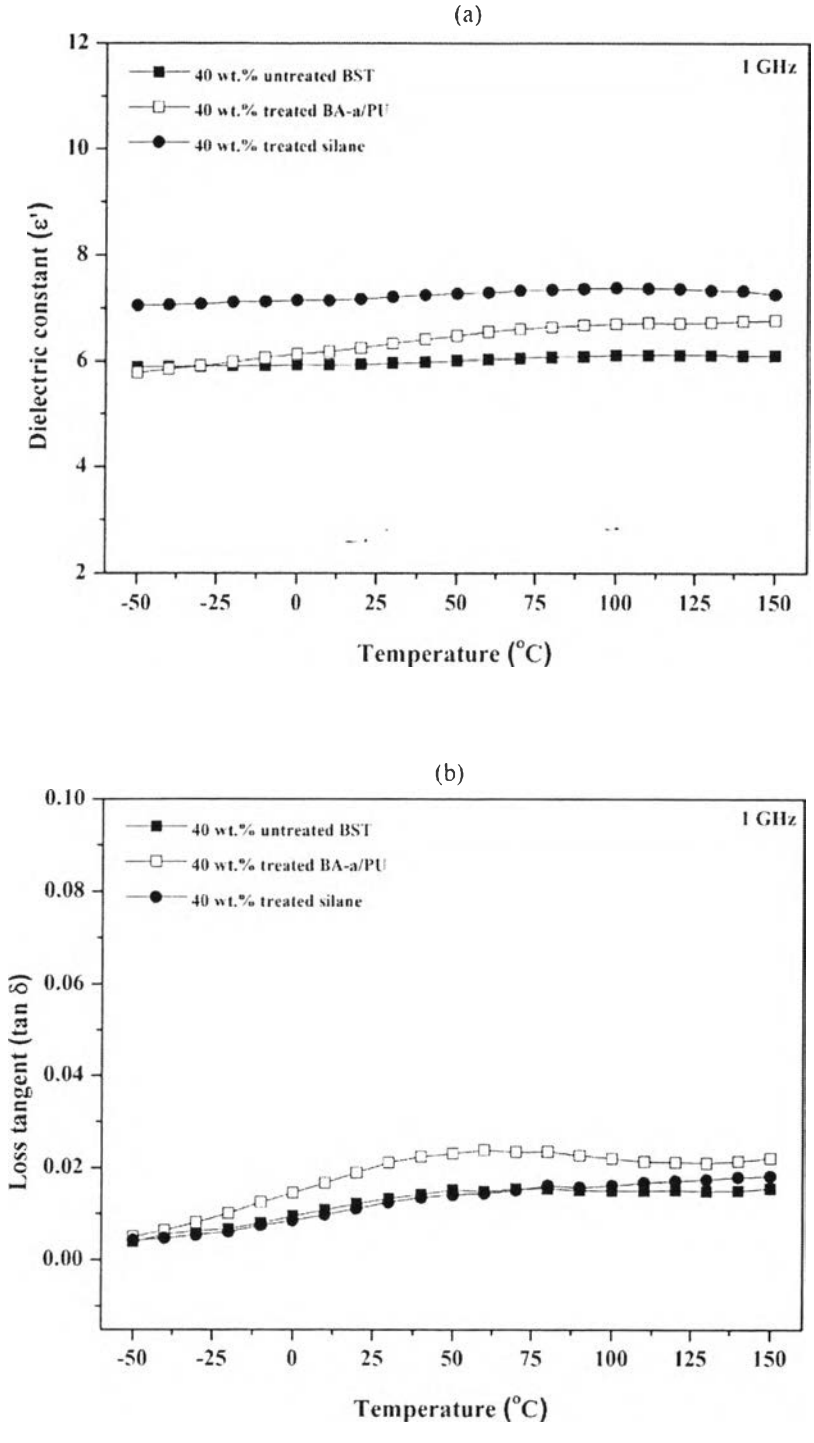

Figure 4.30 Temperature dependence of a) dielectric constant and b) loss tangent of poly(benzoxazine/urethane) composite at 40 wt.% of BST measured at 1 GHz.

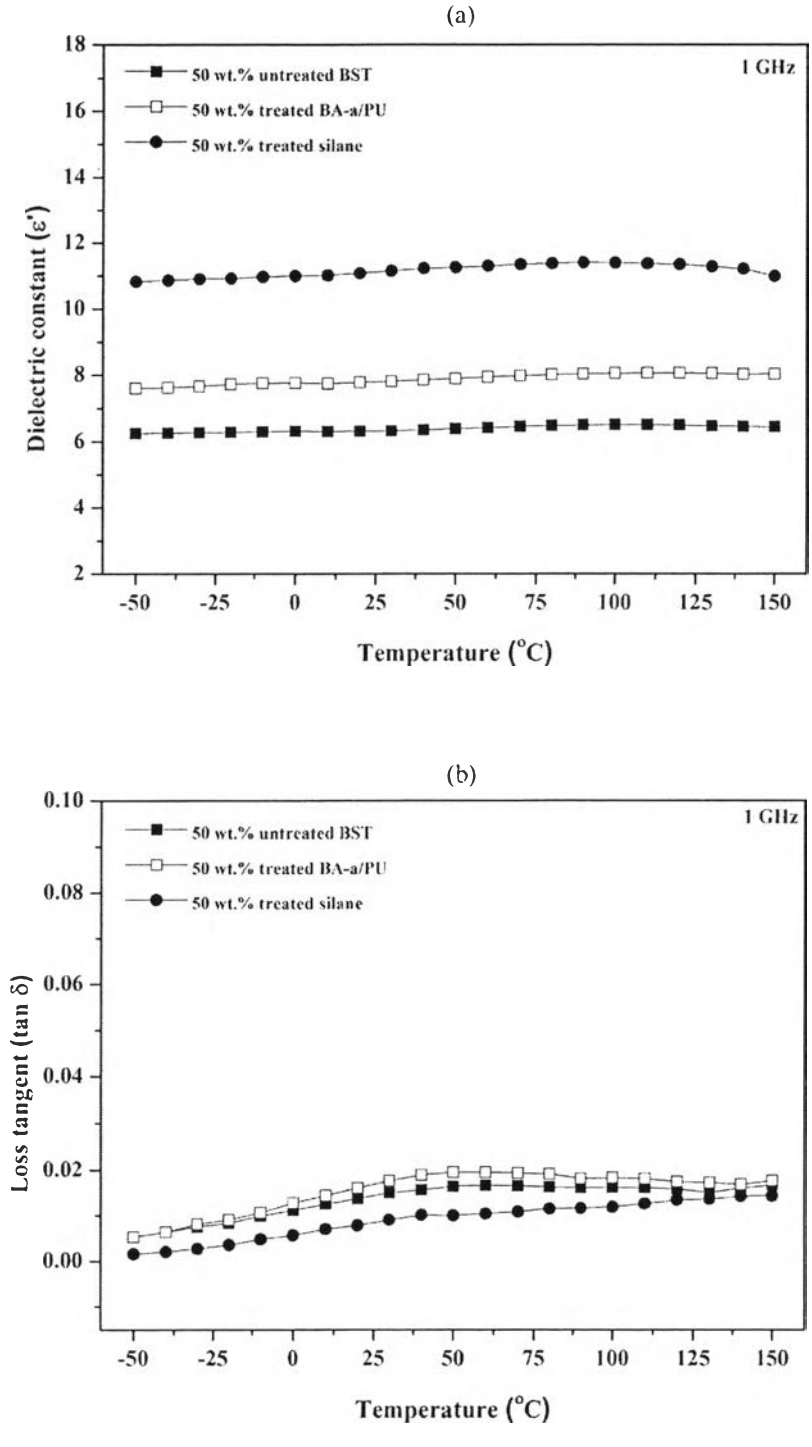

Figure 4.31 Temperature dependence of a) dielectric constant and b) loss tangent of poly(benzoxazine/urethane) composite at 50 wt.% of BST measured at 1 GHz.

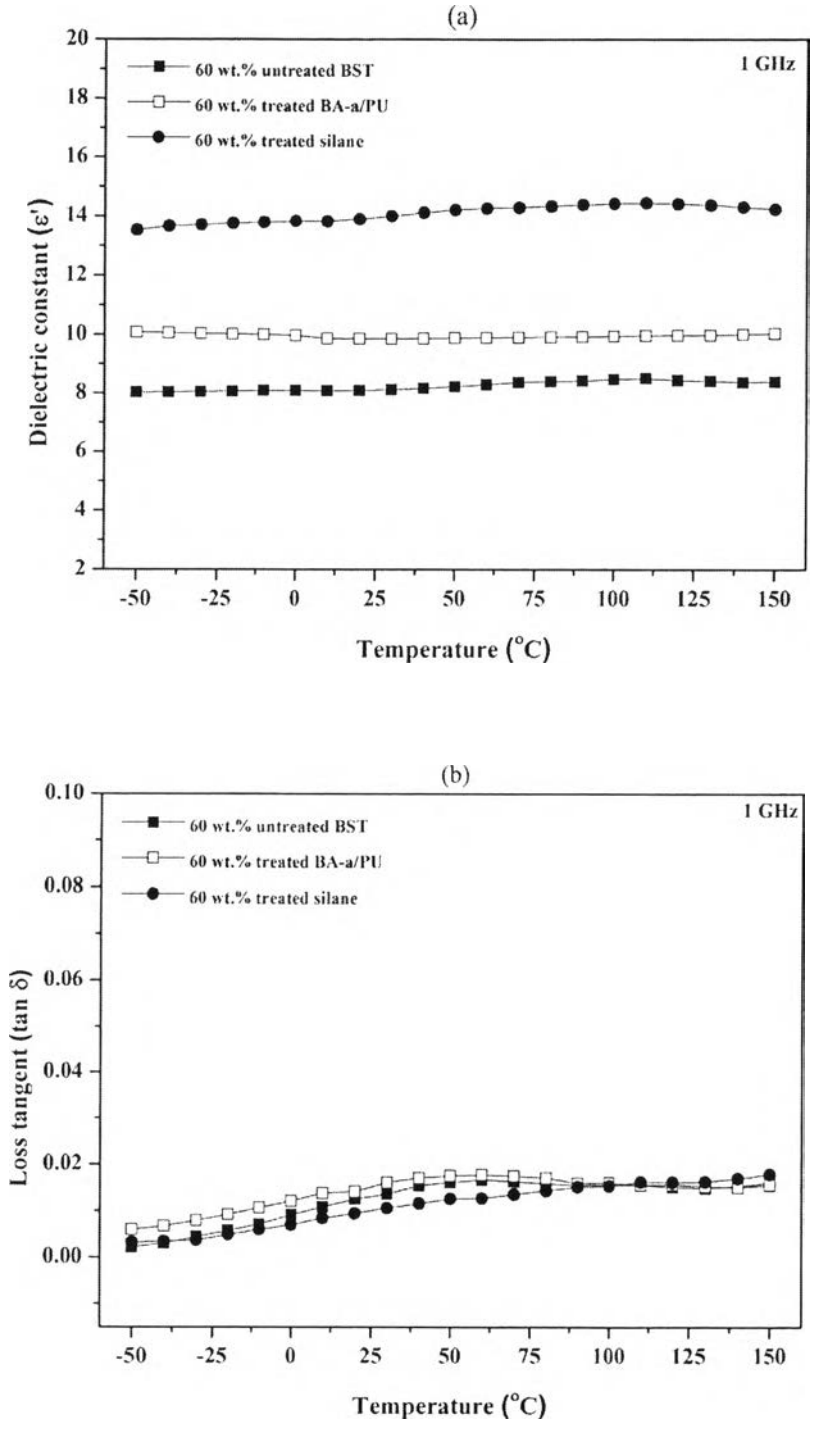

Figure 4.32 Temperature dependence of a) dielectric constant and b) loss tangent of poly(benzoxazine/urethane) composite at 60 wt.% of BST measured at 1 GHz.

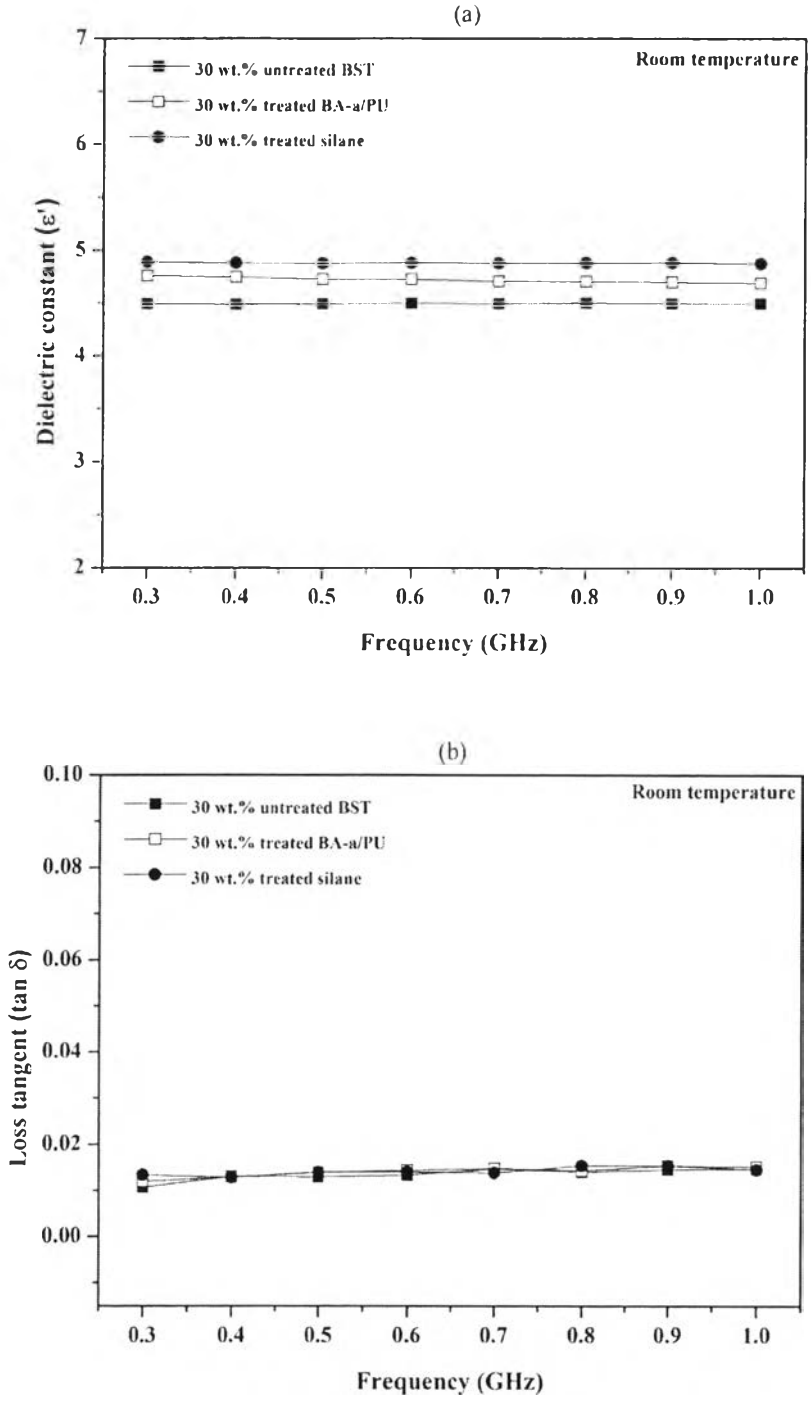

Figure 4.33 Frequency dependence of a) dielectric constant and b) loss tangent of poly(benzoxazine/urethane) composite at 30 wt.% of BST measured at room temperature.

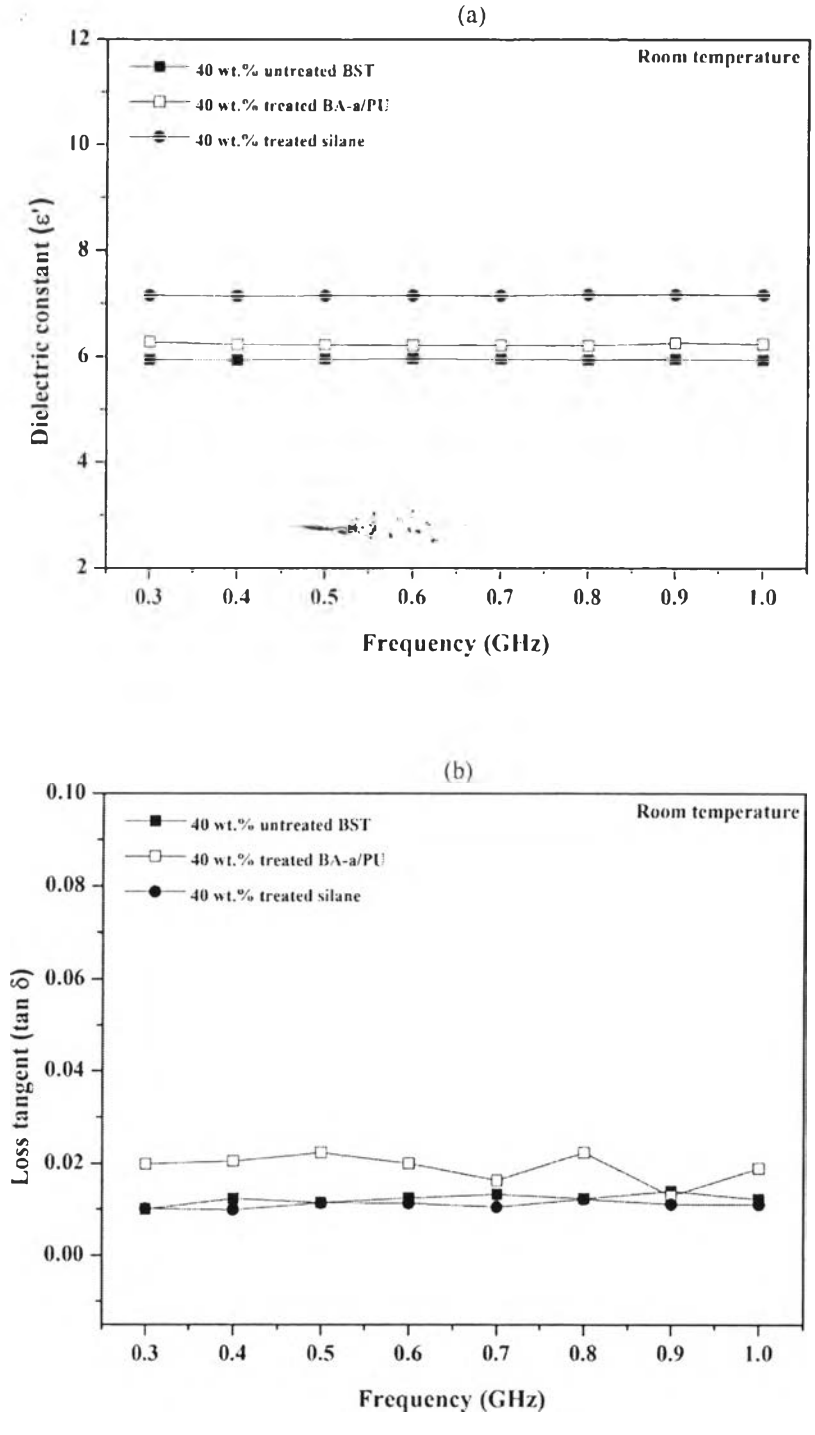

Figure 4.34 Frequency dependence of a) dielectric constant and b) loss tangent of poly(benzoxazine/urethane) composite at 40 wt.% of BST measured at room temperature.

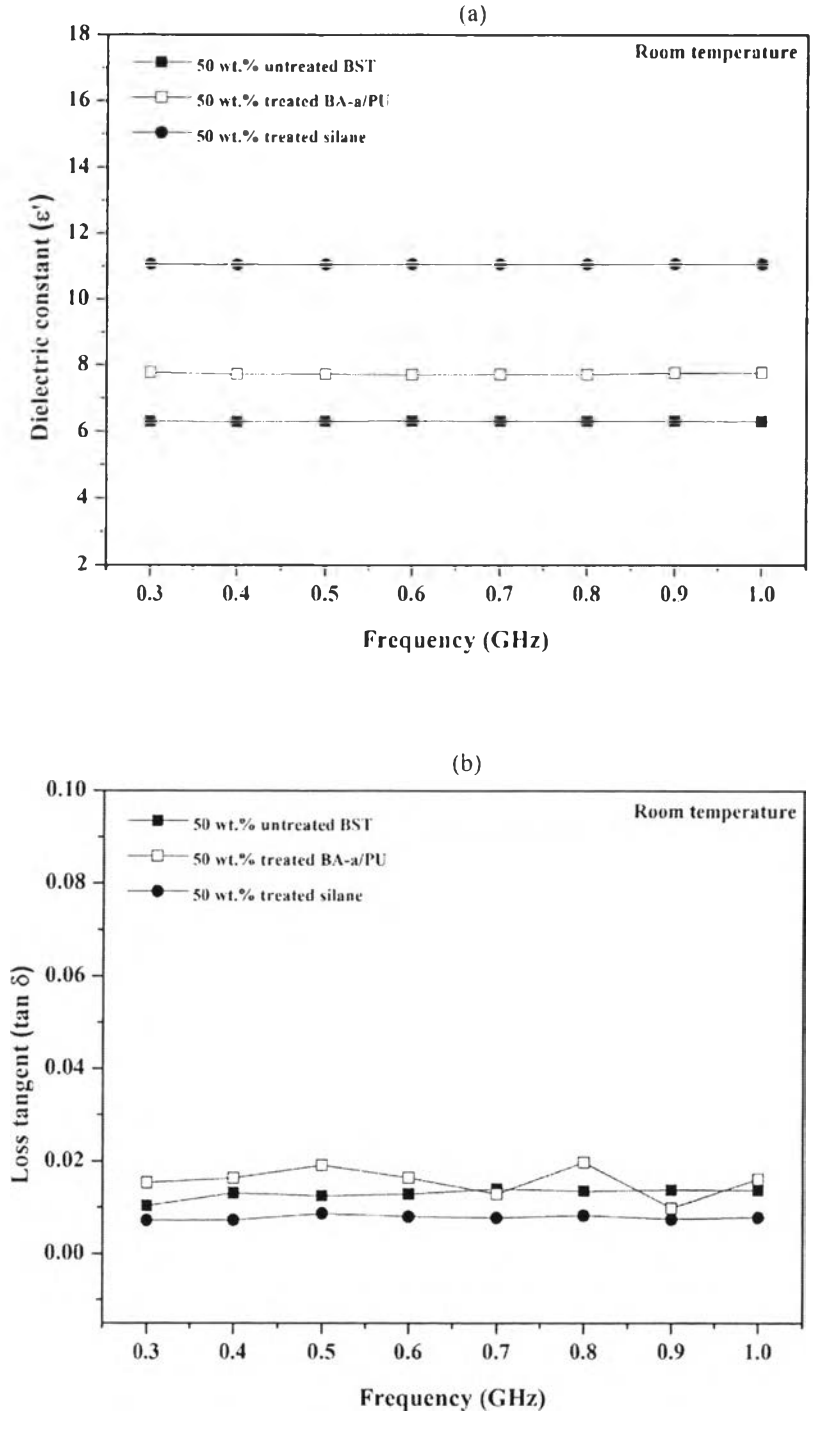

Figure 4.35 Frequency dependence of a) dielectric constant and b) loss tangent of poly(benzoxazine/urethane) composite at 50 wt.% of BST measured at room temperature.

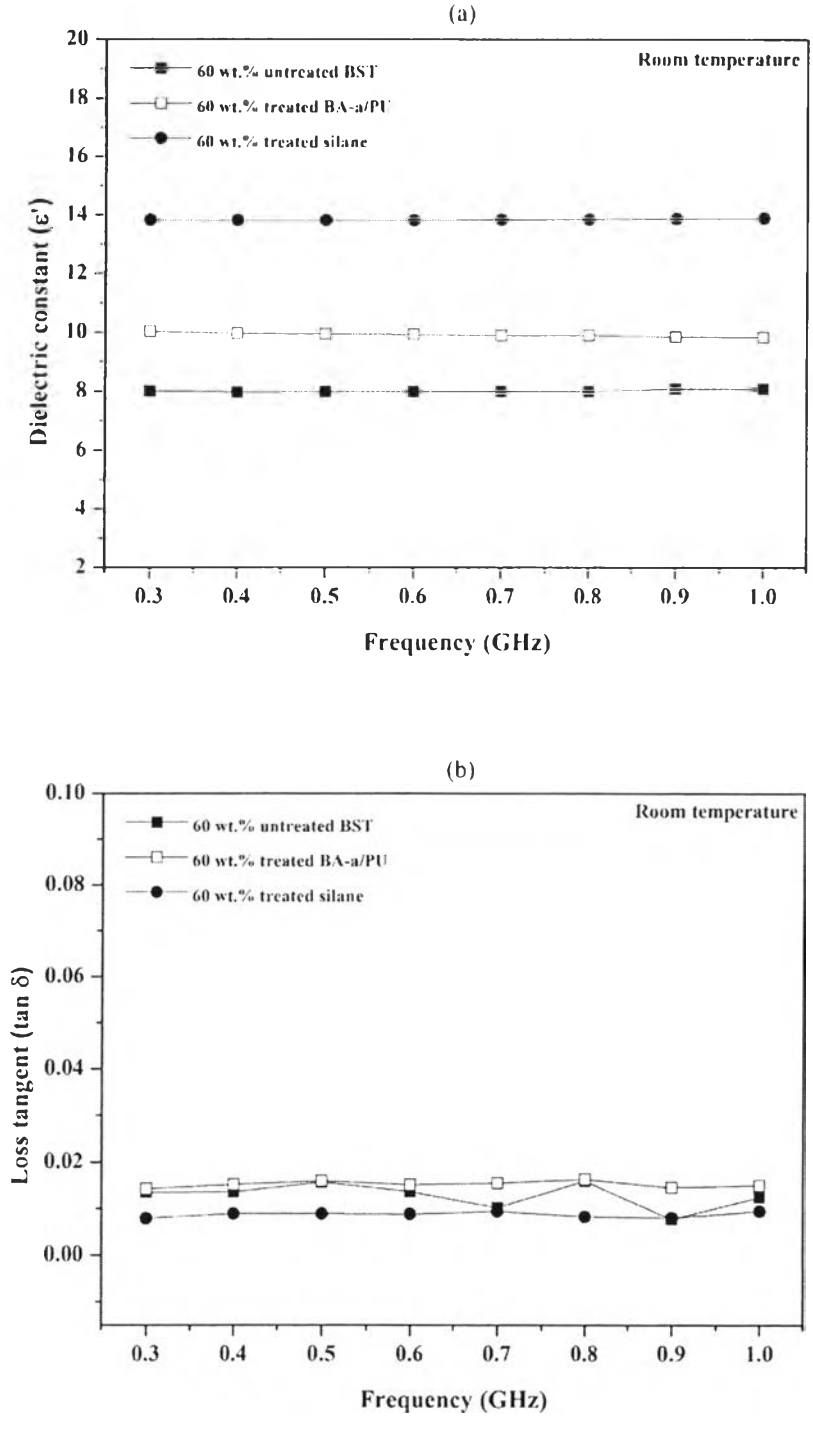

Figure 4.36 Frequency dependence of a) dielectric constant and b) loss tangent of poly(benzoxazine/urethane) composite at 60 wt.% of BST measured at room temperature.

4.5 Conclusions

This research successfully prepared the polymer composites composed of poly(benzoxazine/urethane), (BA-a/PU) and barium strontium titanate, $Ba_{0.3}Sr_{0.7}TiO_3$, (BST) through the melt mixing process. Surprisingly, only a small amount of PU was needed to toughen polybenzoxazine and shifted the dielectric constant of the polymer matrix to a higher value including high thermal stability. At 90/10 (vol.%) BA-a/PU, the polymer matrix yielded the highest permittivity from -50 °C to 150 °C with a low dissipation factor. The microwave dielectric properties of the BA-a/PU composites were studied in relation to the BST loading. The results showed that a higher ceramic content was related to a higher dielectric constant and revealed a slight fluctuation in loss tangent (< 0.0175). For the study of theoretical prediction, the prepared composites were fit well with Lichnecker model at low amount of BST indicated that the composites were a random mixture of nearly spherical inclusion. For higher BST content, Maxwell-Wagner equation was practical for predicting the relative permittivity of the composites suggesting that uniformly distributed spherical inclusions of ceramic material with dielectric constant. In order to solve the incompatibility problem of composites, the surface modification method was proposed. This present work, the surface of BST fillers was treated with 3-aminopropyl-trimethoxy silane and poly(benzoxazine/urethane)base. For this study, the treated composites showed well-dispersed nanophase ceramics in polymer matrix when compared with untreated composites. The dielectric constant of the composite with silane coupling agent was greater than others. The composite at 60 wt.% of silane modified BST predominantly exhibited the highest dielectric constant (13.9) with a low dissipation factor (0.0095) observed at room temperature (1 GHz). Both the loss tangent and especially the dielectric constant of the prepared composites had a weak dependence on frequency (300 MHz to 1 GHz) and temperature, demonstrating low relaxation behaviors. Lastly, the composites in this present work also showed the improvement in thermal stability and stiffness properties which could observe from the higher decomposition temperature and glass transition temperature. It is proved that

poly(benzoxazine/urethane) composites could be an alternative new dielectric materials for microwave frequency applications.

4.6 Acknowledgements

The authors would like to express our deepest gratitude to The Petroleum and Petrochemical College, Chulalongkorn University and the 90th Anniversary of Chulalongkorn University Fund (through the Ratchadaphiseksomphot Endowment Fund) for their financial support.

4.7 References

[1] Sugii, N., Yamada, H., Kagaya, O., Yamasaki, M., Sekine, K., Yamashita, K., Watanabe, M., and Murakami, S. (1998) High-frequency properties of $SrTiO_3$ thin-film capacitors fabricated on polymer-coated alloy substrates. Applied Physics Letters, 72(2), 261-263.

[2] Sebastian, M.T. and Jantunen, H., (2010) Polymer–ceramic composites of 0–3 connectivity for circuits in electronics: A review. International Journal of Applied Ceramic Technology, 7(4), 415–434.

[3] Xie, S.H.,Wei, X. Z., Xu, Z.K., and Xu,Y.Y., (2005) Polyimide/$BaTiO_3$ composites with controllable dielectric properties. Composites: Part A: Applied Science and Manufacturing, 36(8), 1152–1157.

[4] Hu, T., Juuti, J., and Jantunen, H. (2007) RF Properties of BST–PPS composites. Journal of the European Ceramic Society, 27(8-9), 2923–2926.

[5] Kuo, D.H., Chang, C.C., Su, T.Y., Wang, W.K., and Lin, B.Y. (2004) Dielectric properties of three ceramic/epoxy composites. Materials Chemistry and Physics, 85(1), 201–206.

[6] Cho, S.D., Jan, K.W., Lee, J.G., Paik, K.W., and Kim, H. (2005) Epoxy/$BaTiO_3$ composite films and pastes for high dielectric constant and low tolerance embedded capacitors fabrication in organic substrates. Electronics Packaging Manufacturing, IEEE Transactions on, 28(4), 297–303.

[7] Liou, J.W. and Chiou, B.S., (1998) Dielectric tunability of barium strontium titanate/silicone–rubber composite. Journal of Physics: Condensed Matter, 10(12), 2773–2786.

[8] Muralidhar, C. and Pillai, P.C. (1987) Pyroelectric, dielectric, resistivity and hysteresis behavior of barium titanate ($BaTiO_3$)/polyvinylidene fluoride (PVDF) composites and correlation by SEM. Journal of Materials Science Letters, 6(11), 1243–1245.

[9] Krueson, N., Manuspiya, H., Laoratanakul, P., and Ishida, H. (2008) Dielectric properties enhancement in polybenzoxazine composite at multi-frequency range. Advanced Materials Research, 55-57, 105–108.

[10] Ishida, H. and Allen, DJ. (1996) Mechanical characterization of copolymers based on benzoxazine and epoxy. Polymer, 37(20), 4487-4495.

[11] Ardhyananta, H., Kawauchi, T., Ismail, H., and Takeichi, T. (2009) Effect of pendant group of polysiloxanes on the thermal and mechanical properties of polybenzoxazine hybrids. Polymer, 50(25), 5959-5969.

[12] Takeichi, T., Guo, Y., and Agag, T. (2000) Synthesis and characterization of poly(urethane-benzoxazine) films as novel type of polyurethane/phenolic resin composites. Journal of Polymer Science Part A, 38(22) 4165-4176.

[13] Rimdusit, S., Bangsen, W., and Kasemsiri, P. (2011) Chemorheology and thermomechanical characteristics of benzoxazine-urethane copolymers. Journal of Applied Polymer Science, 121(6), 3669-3678.

[14] Ning, X. and Ishida, H. (1994) Phenolic materials via ring-opening polymerization: synthesis and characterization of bisphenol-A based benzoxazines and their polymers. Journal of Polymer Science Part A: Polymer Chemistry, 32(6), 1121–1129.

[15] Kim, H.D. and Isida, H. (2002) Study on the chemical stability of benzoxazine-based phenolic resins in carboxylic acids. Journal of Applied Polymer Science, 79(7), 1207-1219.

[16] Rimdusit, S., Mongkhonsi,T., Kamonchaivanich, P., Sujirote, K., and Thiptipakorn, S. (2008) Effects of polyol molecular weight on properties of benzoxazine–urethane polymer alloys. Polymer Engineering and Science, 48(11), 2238–2246.

[17] Takeichi, T., Guo, Y., and Agag, T. (2000) Synthesis and Characterization of poly(urethanebenzoxazine) films as novel type of polyurethane/phenolic resin composites. Journal of Polymer Science: Part A: Polymer Chemistry, 38(22), 4165–4176.

[18] Takeichi, T. and Guo, Y. (2001) Prepartion and properties of poly(urethane-benzoxaizine)s based on monofunctional benzoxazine monomer. Polymer Journal, 33(5), 437-443.

[19] ASTM D792 – 00: (2000) Standard test methods for density and specific gravity relative density) of plastics by displacement. Annual book of ASTM standard, 8(1), ASTM international, West Conshohocken, PA.

[20] Su, Y. and Chang, F. (2003) Synthesis and characterization of fluorinated polybenzoxazine material with low dielectric constant. Polymer, 44(26) 7989–7996.

[21] Rimdusit, S., Pristpindvong, S., Tanthapanichakoon, W., and Damrongsakkul, S. (2005) Toughening of polybenzoxazine by alloying with urethane prepolymer and flexible epoxy: A comparative study. Polymer Engineering & Science, 45(3), 288-296.

[22] Jamshidi, S., Yeganeh, H., and Mehdipour-Ataei, S. (2010) Preparation and properties of one-pack polybenzoxazine-modified polyurethanes with improved thermal stability and electrical insulating properties. Polymer International, 60(1), 126-135.

[23] Viswanath, R.N. and Ramasamy, S. (1997) Preparation and ferroelectric phase transition studies of nanocrystalline $BaTiO_3$. Nano Structure Materials, 8(2), 155-162, 1997.

[24] Dang, Z.M., Yu, Y.F., Xu, H.P., and Bai, J. (2008) Study on microstructure and dielectric property of the $BaTiO_3$/epoxy resin composites. Composites Science and Technology, 68(1), 171-177.

[25] JS, M. and LokeNgai, K. (2011) Microwave properties of dielectric materials, microstrip antennas. Malaysia: InTech.

[26] Kuo, D.H, Chang, C.C., Su, T.Y., Wang, W.W., and Lin, B.Y. (2001) Dielectric behaviours of multi-doped $BaTiO_3$/epoxy composites. Journal of the European Ceramic Society, 21(9), 1171–1177.

[27] Bai, Y., Cheng, Z.Y., Bharti, V., Xu, H.S., and Zhang, Q.M. (2000) High-dielectric-constant ceramic-powder polymer composites. Applied Physics Letters, 76(25), 3804–3806.

[28] Zhang, J., Xu, R., and Yu, D. (2007) A novel poly-benzoxazinyl functionalized polyhedral oligomeric silsesquioxane and its nanocomposite with polybenzoxazine. European Polymer Journal, 43(3), 743–752.

[29] Du, W., Shan, J., Wu, Y., Xu, R., and Yu, D. (2010) Preparation and characterization of polybenzoxazine/trisilanol polyhedral oligomeric silsesquioxanes composites. Materials and Design, 31(4), 1720–1725.

[30] Agag, T. and Takeichi, T. (2000) Polybenzoxazine–montmorillonite hybrid nanocomposites: synthesis and characterization. Polymer, 41(19), 7083–7090.

[31] Rao, Y., Takahashi, A., Wong, C.P. (2003). Di-block copolymer surfactant study to optimize filler dispersion in high dielectric constant polymer–ceramic composite. Composites Part A: Applied Science and Manufacturing, 34(11), 1113–1116.

[32] Cho, S.D. and Paik, K.W. (2001) Relationships between suspension formations and properties of $BaTiO_3$/epoxy composite films for integral capacitors. Proceedings of the 51st IEEE electronic component technology conference, Piscataway, USA. 1418–1422.

[33] Cho, S.D., Lee, S.Y., Hyu, J.G., and Paik, K.W. (2005) Comparison of theoretical predictions and experimental values of the dielectric constant of epoxy/$BaTiO_3$ composite embedded capacitor films. Journal of Materials Science: Materials in Electronics, 16(2), 77– 84.

[34] Smith, A. (1960) Infrared spectra-structure correlations for organosilicon compounds. Spectrochimica Acta, 16(1-2), 87-105.

[35] Ishida, H. and Podriguez, Y. (1995) Curing kinetics of a new benzoxazine-based phenolic resin by differential scanning calorimetry. Polymer, 36(16), 3151-3158.